catalysts

MDPI

Review

Influence of Impurities in the Chemical Processing Chain of Biomass on the Catalytic Valorisation of Cellulose towards γ-Valerolactone

Preeti Kashyap [1], Magdalena Brzezińska [1,2], Nicolas Keller [2,*] and Agnieszka M. Ruppert [1,*]

[1] Institute of General and Ecological Chemistry, Faculty of Chemistry, Lodz University of Technology, ul. Zeromskiego 116, 90-924 Lodz, Poland; preeti.preeti@dokt.p.lodz.pl (P.K.); brzezinskamm@gmail.com (M.B.)
[2] Institut de Chimie et Procédés pour l'Energie, l'Environnement et la Sante (ICPEES), CNRS, University of Strasbourg, 25 Rue Becquerel, 67087 Strasbourg, France
* Correspondence: nkeller@unistra.fr (N.K.); agnieszka.ruppert@p.lodz.pl (A.R.)

Abstract: The conversion of lignocellulosic biomass to valuable chemicals such as levulinic acid and γ-valerolactone is a promising approach for achieving a sustainable circular economy. However, the presence of impurities during the stepwise chemical processing chain of the biomass feedstock can significantly impact both the hydrolysis and hydrogenation steps implemented to convert the cellulosic feedstock to levulinic acid and further to γ-valerolactone, respectively. This review article explores the effects of those impurities by classifying them into two groups, namely endogenous and exogenous types, based on whether they originate directly from the raw lignocellulosic biomass or arise during its multi-step chemical processing. Endogenous impurities include heavy metals, alkali metals, alkaline earth metals, proteins, and side products from the downstream treatment of cellulose, while exogenous impurities are introduced during physical pre-treatments such as ball milling or during the hydrolysis step, or they might originate from the reactor setup. The specific catalyst deactivation by carbonaceous species such as humins and coke is considered. The mechanisms of impurity-induced catalyst deactivation and by-product formation are thoroughly discussed. Additionally, strategies for minimizing the detrimental effects of impurities on biomass conversion and enhancing catalytic efficiency and stability are also proposed.

Keywords: impurities; lignocellulosic biomass; levulinic acid; γ-valerolactone; catalyst deactivation; heterogeneous catalyst

Citation: Kashyap, P.; Brzezińska, M.; Keller, N.; Ruppert, A.M. Influence of Impurities in the Chemical Processing Chain of Biomass on the Catalytic Valorisation of Cellulose towards γ-Valerolactone. *Catalysts* **2024**, *14*, 141. https://doi.org/10.3390/catal14020141

Academic Editor: Francesco Mauriello

Received: 11 January 2024
Revised: 2 February 2024
Accepted: 7 February 2024
Published: 12 February 2024

1. Introduction

The depletion of fossil fuel reserves associated with the necessity of lowering worldwide CO_2 release presents us with the challenge of finding renewable sources of both chemicals and fuels, as well as elaborating sustainable chemical processing for their production. One of the most promising candidates is the abundant lignocellulosic biomass feedstock, i.e., the so-called biomass of second generation, that is based on the waste fraction of plants and, as a consequence, is characterized by its lack of competition with the food industry. It is expected to play a pivotal role in the move towards future renewables-based biorefinery schemes [1,2].

Lignocellulosic biomass consists of three main components, namely cellulose, hemicellulose, and lignin (Figure 1). Cellulose is the predominant component, while both cellulose and hemicellulose account for ca. 50–85% of the overall weight depending on the biomass source. In terms of chemical composition, cellulose is a high molecular weight crystalline polysaccharide $(C_6H_{12}O_6)_n$ composed only of D-glucose (C_6) units linked with β-1,4-glycosidic bonds, whereas hemicellulose is built with different monosaccharide units, namely pentoses and hexoses, linked together via α-1,2- and β-1,4-glycosidic bonds [3]. Unlike cellulose, hemicellulose consists of 50–3000 sugar units as opposed to

7000–15,000 glucose molecules per polymer in cellulose. In both cases, the amount of the sugar monomers changes quite dramatically for different feedstock sources. The last form, lignin, is an aromatic 3D network of linked phenylpropane sub-units. By contrast to cellulose, which exhibits a strong crystalline structure and is resistant to hydrolysis, hemicellulose and lignin are amorphous structures that both originate from the plant cell walls [4]. However, lignocellulosic biomass also comprises other components that cannot be omitted, among which we find proteins, ash, extractives, and starch [5].

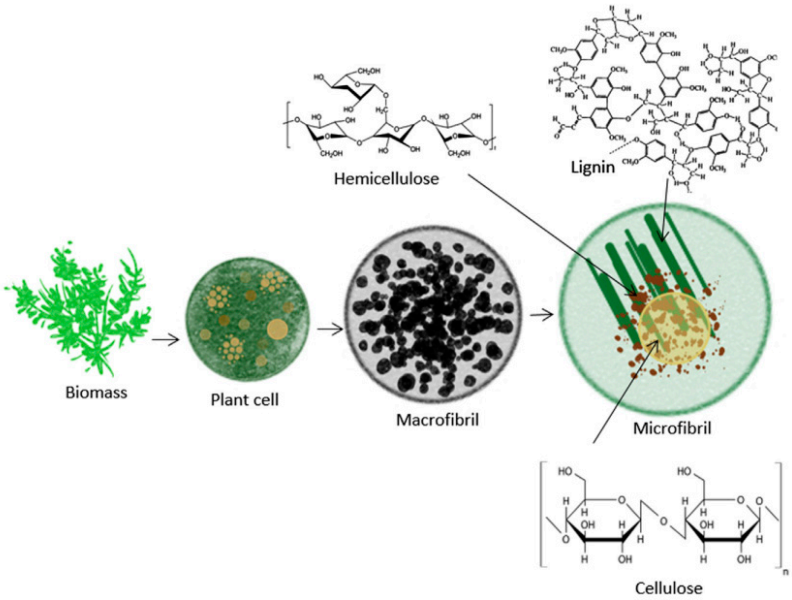

Figure 1. Main components of lignocellulosic biomass. Reproduced with permission from M. Jędrzejczyk et al., J. Physical and Chemical Pretreatment of Lignocellulosic Biomass; published by Elsevier, 2019, [6].

The strongly variable content of the lignin component (10–50 wt%, as nominally $C_9H_{10}O_3$) is responsible for practical issues associated with the feedstock inhomogeneity, in addition to a greater degree of intractability in pre-treatment due to its aromatic (hydrophobic) qualities [7].

One of the most promising intermediates (platform molecules) that can be processed from the cellulose fraction, and in particular from the dehydration of C-6 carbohydrates, is levulinic acid (LA), used as a building block for the synthesis of many high added value chemicals [8]. The chemical processing of lignocellulosic biomass requires the implementation of a series of non-catalytic and catalytic processes to produce high added value compounds, and in particular the valuable LA platform molecule, that can be further converted into a wide span of valuable chemicals. Among them, γ-valerolactone (GVL) gained significant attention because of its versatile applications; for instance, it can be used as a solvent or precursor in chemical synthesis, or as biofuel or biofuel additive due to its low volatility, minimum toxicity, and good stability [9–11].

However, like in most industrial (chemical) processes, the efficiency of many transformation steps in the chemical processing chain of biomass appears to be affected by the presence of impurities, whether from the conversion of the initial biomass feedstock or the further conversion of biomass-derived molecules. In particular, it is well known that the heterogeneous catalysts used during the stepwise conversion chain are susceptible to deactivation, due to their poisoning by the impurities present in the reaction media. Gaining deeper knowledge on the origin of impurities and their impact on catalyst performance and more globally on the biomass conversion process chain remains, therefore, of prime importance in the search for more performant and more robust catalysts and in the understanding of the reaction mechanisms.

To this end, this review aims to describe the influence of the span of impurities that are present during the stepwise chemical processing of lignocellulosic biomass. First, the main physical and chemical pre-treatments directly applied to the raw lignocellulosic biomass feedstock are itemized in Section 2, together with the subsequent catalytic processing of the biomass. Section 3 discriminates endogenous and exogenous impurities depending on the way they are introduced into the chemical processing chain of biomass. Sections 4 and 5 report on the influence of the so-called endogenous and exogenous impurities on the efficiency of the biomass and biomass-derived molecules conversion processes, while the deactivation of catalysts by carbonaceous species such as humins and coke is reviewed in Section 6. Future perspectives directly deriving from the key aspects associated to the influence of impurities are finally emphasized.

2. Lignocellulosic Biomass Processing

The initial processing of biomass usually consists of the fractionation of the polymers. Therefore, the first step of biomass processing aims to isolate the biomass fractions and increase the cellulose susceptibility in order to consequently facilitate its depolymerisation and solubilisation [12]. This first step is realized by chemical or physical pre-treatments and/or combinations thereof, namely, e.g., mechanical, hydrothermal (steaming), chemical (hydrolysis), and biochemical (enzymatic saccharification) processes. The main pre-treatment methods are summarized in Figure 2.

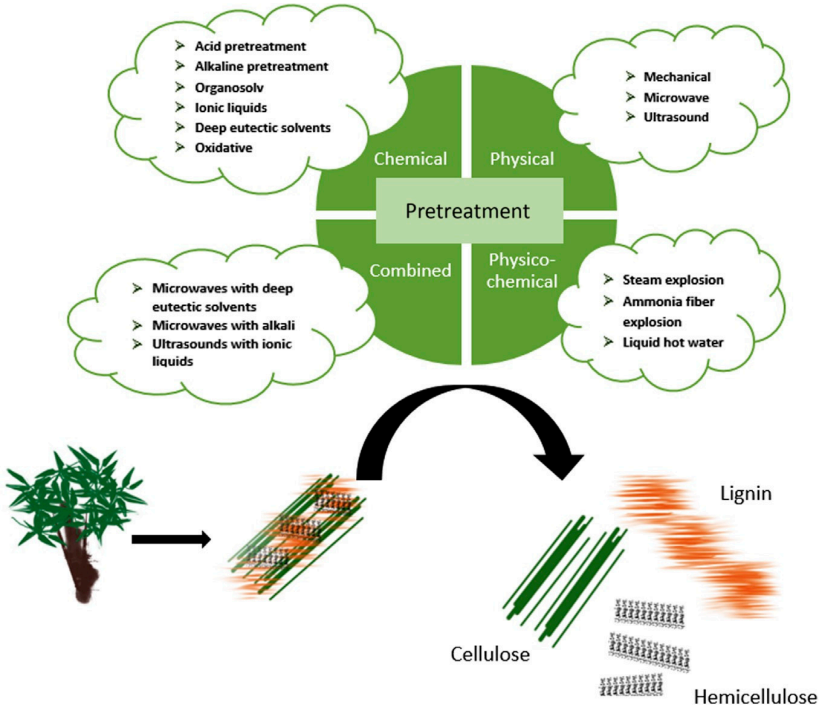

Figure 2. Different methods of lignocellulosic biomass pretreatment. Reproduced with permission from M. Jędrzejczyk et al., J. Physical and Chemical Pretreatment of Lignocellulosic Biomass; published by Elsevier, 2019, [6].

2.1. Physical Pre-Treatments

Physical pre-treatment aims to unify the macrostructure of the biomass, destroy its crystalline structure, and increase its specific surface area, in order to separate lignin and to make hemicellulose and cellulose more accessible to chemicals. To accomplish that goal, biomass is subjected to different types of physical processes [6], e.g.,:

- Milling or grinding,
- Chipping,
- Extrusion,

- Processes applied under irradiation (microwave) or ultrasound excitation.

2.2. Chemical Pre-Treatments

Chemical pre-treatments include globally a wider span of processes in comparison to physical pre-treatments, that can be itemized as follows [6,13]:

- Hydrothermal pre-treatments in hot water at elevated temperatures (120–230 °C) [14,15].
- Acid pre-treatments, notably using hydrochloric, sulfuric, formic, and acetic acids [16,17]. The so-called Organo Cat process operates in particular in a biphasic water/bio-based 2-MeTHF solvent system using oxalic acid as catalyst [18].
- Alkali pre-treatments at room temperature using bases such as NaOH, KOH, $Ca(OH)_2$, or anhydrous ammonia [19–21]. Kraft pulping alkaline treatment has recently attracted attention [22].
- Treatments with ILs or eutectic liquids include mainly imidazolium-based, alkylammonium-based, and lignin-derived phenol-based ILs [23,24].
- Oxidative pre-treatments use reagents like hydrogen peroxide (H_2O_2), oxygen, air, and peroxyacid [21,25,26].
- Pre-treatments using a span of organic solvents with or without the addition of a catalyst, that are referred under a common umbrella as Organosolv processes [27].
- Steam explosion pre-treatments that expose the biomass to saturated steam with high pressure and rapidly drop pressure, causing the materials to decompress explosively with the disruption of H bonds and glycosidic links [28,29].

The main chemical pre-treatment methods are summarized in Figure 3.

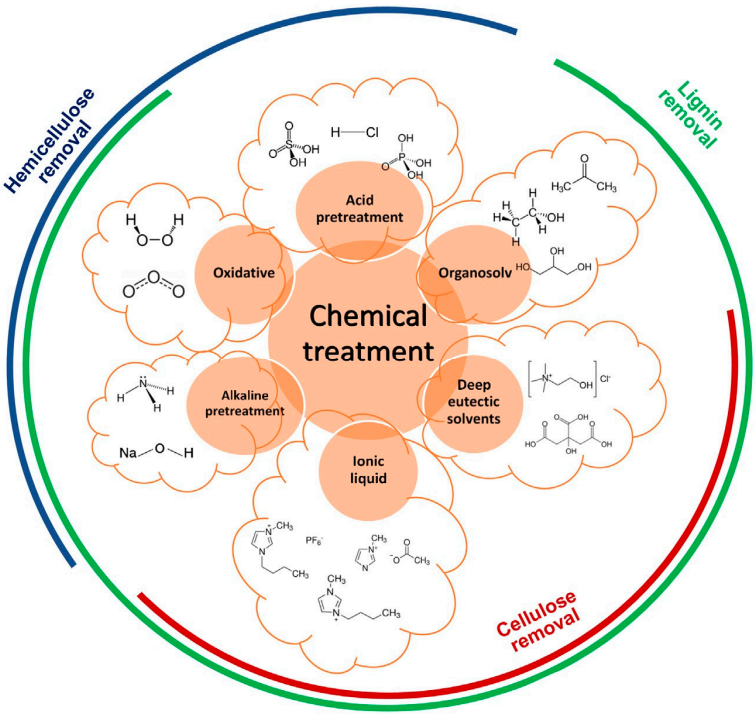

Figure 3. Visual presentation of different methods of chemical pretreatment. Reproduced with permission from M. Jędrzejczyk et al., J. Physical and Chemical Pretreatment of Lignocellulosic Biomass; published by Elsevier, 2019, [6].

2.3. Catalytic Chemical Processing of Lignocellulosic Biomass

In general, as depicted in Scheme 1, the chemical processing of lignocellulosic biomass gives rise to two different pathways for producing the valuable platform molecule that is LA. The dehydration of hexose sugars in the presence of diluted acid allows to obtain HMF, while pentose sugars are dehydrated into furfural (FFR) which is further hydrogenated,

leading to the formation of furfuryl alcohol. The acidic hydrolysis of furfuryl alcohol also results in obtaining LA [30]. LA can be produced through various means, one of which involves the heating of hexose or hexose-containing carbohydrates with a weak mineral acid over an extended period [31]. However, a significant drawback of this approach is the challenge of separating the resulting products from the acidic reaction mixture. As an alternative method, heterogeneous catalysts such as supported metal catalysts, ion exchange resins, or zeolites can be employed. However, the disadvantage of this method lies in the low product yields of the reaction, so that long reaction times are necessary to obtain reasonable quantities of LA.

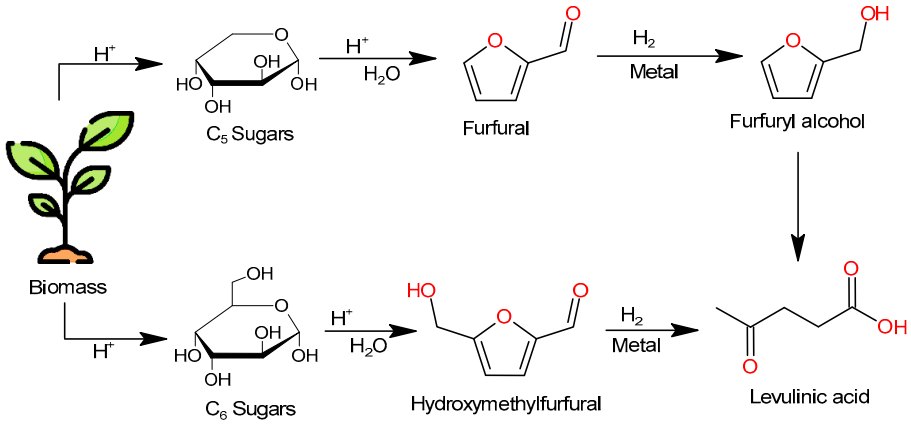

Scheme 1. Conversion pathway of biomass to levulinic acid.

Further, the catalytic (upgrade) conversion of LA into GVL is reported to occur via two pathways, namely via 4-hydroxypentanoic acid (HPA) or α-angelica lactone (AL) intermediates (Scheme 2). The HPA reactional pathway initiates first with the hydrogenation of the carbonyl group of the LA to form the HPA intermediate which is further dehydrated with both esterification and ring closure to obtain GVL. By contrast, the alternative pathway takes place first with the dehydration of LA with ring closure to form the LA intermediate, which subsequently undergoes C=C bond hydrogenation to obtain GVL [32]. The HPA pathway occurs in mild conditions and is therefore proven to be thermodynamically preferred [33]. Furthermore, in the context of liquid-phase hydrogenation using metal-supported catalysts, it is reported that the reaction of LA progresses through HPA as an intermediate [33,34]. On the other hand, when hydrogenation takes place in the vapor phase, it results in the formation of α-angelica lactone [35,36].

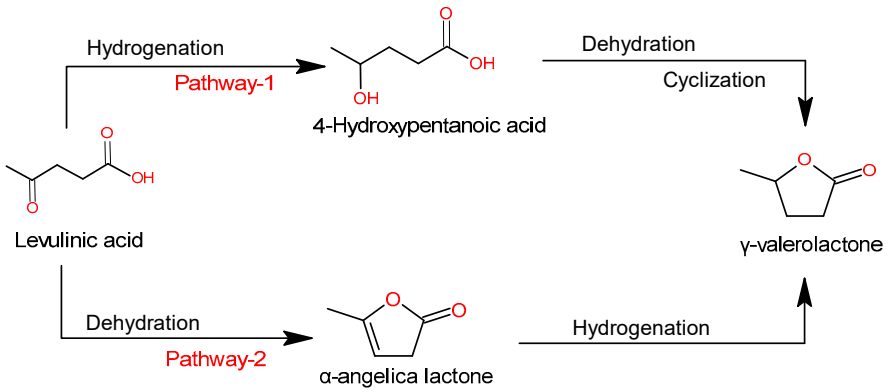

Scheme 2. Levulinic acid hydrogenation pathways towards γ-valerolactone.

LA hydrogenation is conducted mainly in the presence of a pressurized external source of hydrogen. However, there are also interesting examples of LA hydrogenation with an internal source of hydrogen such as an alcohol or formic acid (FA) [37]. It is important to

highlight that the hydrogenation of LA has been the subject of intensive research, with numerous evaluations of various heterogeneous catalysts using commercially available high purity reactants, both in liquid and gas phases [34,37]. Often, however, high purity chemicals were usually used, and the presence of possible impurities related to the reaction environment was not considered.

3. Categorization of the Origin of the Biomass Impurities

The primary origin of the impurities present during the processing chain of cellulose conversion can be categorized into two groups, namely endogenous and exogenous (Figure 4).

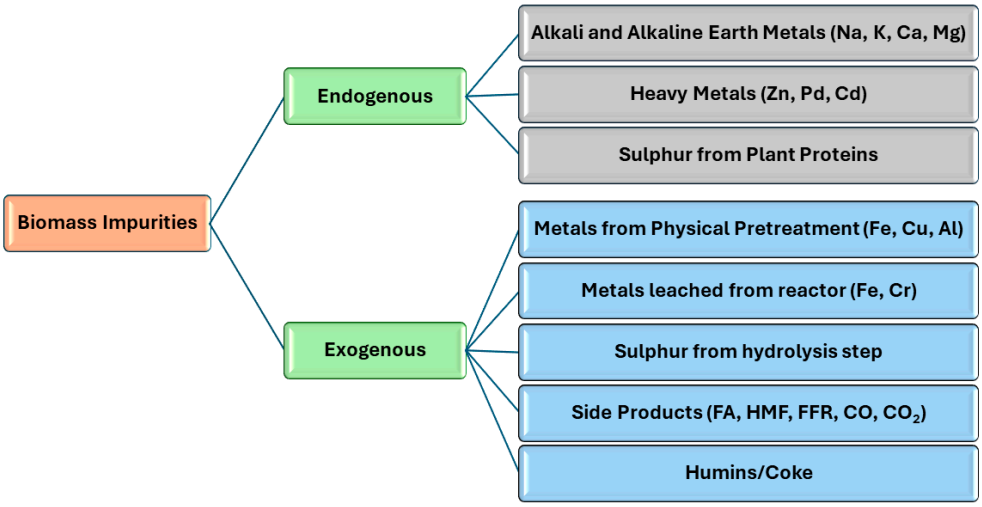

Figure 4. Classification of the presence of impurities in biomass conversion.

Endogenous impurities originate directly from the raw lignocellulosic biomass and involve a diverse array of inorganic and organic components, such as heavy metals present in the biomass or introduced, e.g., through phytoremediation, amino acids as part of the plant cell structure, and various minerals. They are present before any physical or chemical treatment, directly tied to the diverse composition of the biomass.

In contrast, exogenous impurities arise during the multi-step processing of biomass. Physical pre-treatments, such as milling or grinding, contribute to exogenous impurities through contact with the processing equipment. The hydrolysis step introduces impurities from both heterogeneous catalysts (e.g., sulfonated polymer resins), that are susceptible to leaching phenomena, and from homogeneous catalysts (e.g., H_2SO_4, HCl), which may introduce foreign ions. The corrosive nature of the environment further contributes to the introduction of impurities from the reaction setup. Additionally, impurities can be introduced during the subsequent conversion of the obtained hydrolysate. Therefore, the discussions about these issues emphasize the importance of managing impurities at different stages to enhance the process efficiency as well as the purity of the final product in LA conversion.

The prime importance of studying the direct impact of both exogeneous and endogenous impurities on the ability of catalysts to hydrogenate LA into GVL with high yield is well substantiated in Table 1, which itemizes selected examples demonstrating that the GVL yield faces a substantial drop in presence of different types of impurities.

Table 1. Effect of different impurities on LA hydrogenation towards GVL.

Catalyst	Reaction Temperature (°C)	Solvent	H_2 Pressure [bar]	Reaction Time [h]	Impurity Type	GVL Yield [%] without Impurities	GVL Yield [%] with Impurities	Ref.
Ru(5%)/C	150	dioxane	50	1	0.025 wt% H_2SO_4	93	48	[38]
Ru(5%)/C	150	dioxane	50	1	0.05 wt% H_2SO_4	93	10	[38]
Ru(5%)/C	150	water	35	20	0.5 mol L^{-1} H_2SO_4	98	60	[39]
Ru(1%)/ZrO_2	150	dioxane	50	3	0.25 wt% H_2SO_4	47	3	[38]
Ru(1%)/ZrO_2	150	dioxane	50	15	0.5 wt% H_2SO_4	90 [b]	12 [b]	[40]
Ru(1%)/ZrO_2	90	water	50	20	0.5 wt% H_2SO_4	95 [b]	75 [b]	[40]
Ru(1%)/TiO_2	150	dioxane	50	15	0.5 wt% H_2SO_4	95 [b]	10 [b]	[40]
Ru(1%)/TiO_2	90	water	50	20	0.5 wt% H_2SO_4	95 [b]	80 [b]	[40]
Ru(5%)/ZrO_2	30	water	50	1	0.9 wt% H_2SO_4 + HCOOH	91	0	[41]
Ru(1%)/ZrO_2	150	dioxane	50	1	Cysteine (Cys) [a]	100 [b]	12 [b]	[40]
Ru(1%)/ZrO_2	150	dioxane	50	1	Metheonine (Meth) [a]	100 [b]	48 [b]	[40]
Ru(5%)/TiO_2	190	water	20	1	1 µg Zn	98	44	[42]
Ru(1%)/TiO_2	170	water	50	5	Humins	31	6	[43]
Ru(1%)/TiO_2	150	dioxane	50	1	0.5 wt% humins	90 [b]	53 [b]	[40]
Ru(1%)/ZrO_2	150	dioxane	50	1	0.5 wt% humins	90 [b]	50 [b]	[40]
Ru(5%)/C	150	water	40	1	2 mmol HCOOH	67	2	[44]
Ru(1%)/ZrO_2	150	dioxane	50	10	0.5 wt% HCOOH	90 [b]	0 [b]	[40]
Ru(1%)/ZrO_2	90	water	50	10	0.5 wt% HCOOH	99 [b]	10 [b]	[40]
Ru(1%)/TiO_2	150	dioxane	50	10	0.5 wt% HCOOH	98 [b]	3 [b]	[40]
Ru(1%)/TiO_2	90	water	50	10	0.5 wt% HCOOH	90 [b]	3 [b]	[40]

[a] Cys or Meth to LA ratio = 1:500, [b] GVL + HPA yield (HPA = 4-hydroxypentanoic acid).

4. Biomass Endogenous Impurities

Endogenous impurities from the biomass processing chain are considered to mainly originate from soil and directly from plant proteins. The category of endogenous impurities also includes by- and co-products resulting from the initial hydrolysis of biomass and other competitive reactions.

4.1. Impurities from Soil Origin

Soils are very prone to any type of contamination coming both from hydrological (study of water on and below the earth's surface) and atmospheric sources. In the case of highly polluted soils such as in post-mine or post-industrial areas, they might contain many impurities of different natures like heavy metals (e.g., As, Cd, Hg, Mo, Pb). Soil pollution is one of the serious environmental concerns of today's world. It is a growing problem causing vast areas of land to become unexploited and hazardous for both wildlife and human beings, directly on-site or indirectly by impacting vital ecosystems [45]. High concentrations of heavy metals are present in soils in the surrounding mines due to the dispersion of mine waste materials into nearby soils. Metals/metalloids present in such polluted soils can be dispersed downstream due to the weathering and erosion processes of

tailings. The extent and degree of heavy metal contamination can be significant over vast areas, which causes a major impact on the environment.

4.1.1. Phytoremediation Processes

In order to diminish the negative impact of soil-originating impurities, the phytoremediation process is one of the actions undertaken, which consists of taking advantage of plants' accumulation properties to remediate the polluted soil. Phytoremediation is a process in which living plants are used to reduce the mobility, toxicity, or volume of the pollution in the soil, groundwater, or other contaminated media, so that plants may clean up many kinds of pollution such as heavy metals, pesticides, or oil. While the phytoremediation strategy depends on the types of impurities present and on the soil properties, phytoremediation is a generic term for plant-mediated cleaning processes independent of their action mechanisms, namely phytoextraction, rhizofiltration, phytovolatilization, phytostabilization, phytodegradation, hydraulic control, or rhizodegradation (Figure 5).

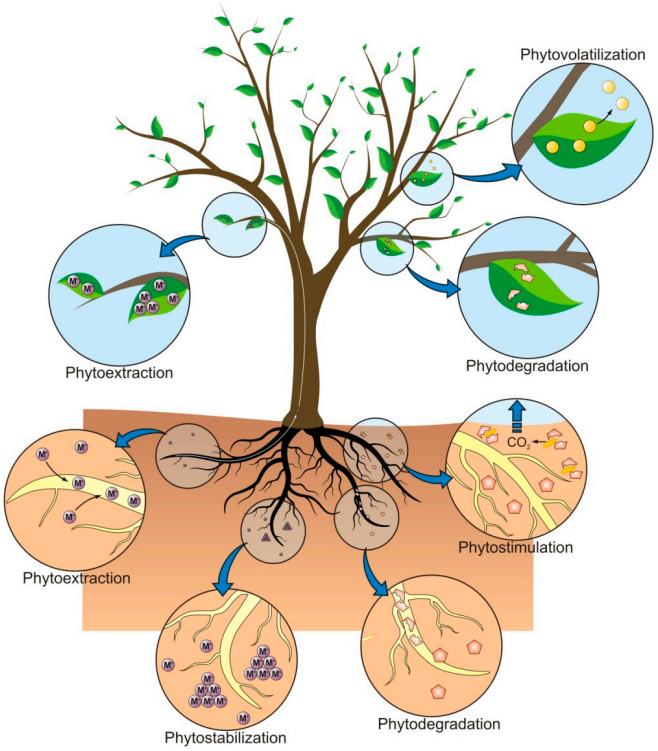

Figure 5. Overview of the main phytoremediation processes. Reproduced from Favas et al., Phytoremediation of Soils Contaminated with Metals and Metalloids at Mining Areas: Potential of Native Flora, in: Environmental Risk Assessment of Soil Contamination; published under the Creative Commons CC-BY-3.0 license by IntechOpen Ltd, 2014, [46].

Phytoremediation usually operates through one of the first three mechanisms mentioned above in the case of heavy metals. For example, the phytoextraction strategy that involves contaminant absorption by the plant roots followed by translocation and accumulation in other parts of the plants is often used for metals and metalloids (like Cd, Ni, Cu, Zn, Pb, and As) as well as for the removal of organic compounds. In this case, plants known as hyperaccumulators are often applied, as they have the ability to store high concentrations of metals (0.01% to 1% of the dry weight, depending on the metal). The latter three strategies are used when the soil is polluted with organic molecules such as hydrocarbons, aromatic hydrocarbons, chlorinated solvents, or pesticides [47]. The accumulation of inorganic compounds in soil over an extended period has the potential to reduce soil pollutants, but the high concentration of these impurities in plants limits their use. Currently, various strategies are being developed to use these plants as feedstock

for multiple synthesis, enhancing sustainability but also introducing new challenges related to inorganic impurities. The content of these impurities (presented as ash content) can be substantial in the biomass, for example, rice husks contain around 10% ash, and sludge biomass might contain around 19% [48]. Biomass ash commonly contains silicates, sulphates, phosphates, carbonates, chlorides, and nitrates, with silica being consistently recognized as the most abundant inorganic component [49,50]. The specific composition of ash depends on factors such as the biomass type and the combustion method, as well as both transport and storage conditions [51].

Even though there are some similarities between coal and biomass, we cannot apply coal conversion technologies directly to biomass conversion. Various studies showed that the biomass composition varies significantly from coal and among different types of biomasses. Biomass generally contains higher levels of certain elements compared to coal. For example, coal contains a maximum of 27.7, 4.1, 3.9, and 16.4 ppm of CaO, K_2O, MgO, and Fe_2O_3, respectively. However, woody and agricultural biomasses contain the same impurities in an amount of 83.5, 31.9, 14.5, 9.5 ppm, and 44.3 63.9, 16.2, and 36.2 ppm, respectively. Factors influencing biomass composition include plant type, growth conditions, geographic location, climate, and harvesting techniques [7]. Despite the potential of biomass as a raw material for synthesizing valuable compounds, the presence of these inorganic impurities poses challenges. These impurities can significantly impact both hydrolysis and hydrogenation processes. Unfortunately, most documented studies on the conversion of biomass-derived molecules have primarily utilized commercial substrates rather than molecules directly derived from lignocellulosic feedstocks. This oversight is crucial, especially in processes involving waste feedstocks, where various impurities can significantly affect catalyst performance.

4.1.2. Impurities Affecting the Hydrolysis and Hydrogenation Steps

Homogenous catalysts like H_2SO_4 and HCl prove to be sufficiently effective in biomass hydrolysis because they can easily penetrate to the complex, heterogeneous structure of cellulose [52]. However, the presence of possible impurities originating from soil can affect their performance.

Soszka et al. conducted a study on the influence of impurities and the nature of biomass feedstock in biomass hydrolysis on the yield to LA. They identified various metal impurities like Cu, Zn, Pb, and Cd in the biomass feedstock. Among these impurities, Zn was found to be the most abundant in the investigated lignocellulosic biomasses [42]. In addition to these impurities, the biomass also contained salts of metals like K, Ca, and Mg. The concentration of these impurities varied depending on the type of biomass and its plant part [7]. Generally, softwoods like pine exhibit lower impurity levels, while hardwoods like birch have higher concentrations [53].

For example, calcium ions can negatively affect the sulphuric acid concentration in the solution. Indeed, insoluble calcium sulphate can precipitate even when sulphuric acid is used in low concentrations (0.005–1 M), leading to reactor clogging during the biomass hydrolysis process [38,42,54]. It was reported that calcium ions combined with the presence of the Fe-based impurities were responsible for decreasing the yield to sugar during hydrolysis. It was found that the presence of Ca and Fe ions in the solution greatly reduced the concentration of tungstate ions in the liquid, because of the formation of insoluble $CaWO_4$ and $FeWO_4$ salts, respectively [55].

Not only calcium ions are identified as harmful. Cao showed that in the absence of any additional catalysts during the hydrolysis of cellulose, both Cu^{2+} and Fe^{3+} ions can catalytically boost the hydrolysis of cellulose to glucose and its further conversion towards LA and FA when the reaction is conducted at high temperatures such as 200 °C [56]. Pang et al. performed cellulose hydrolysis with tungsten-based catalysts in the presence of AlO^{2-} and SiO_3^{2-} impurities and observed that the cellulose conversion decreased strongly. The presence of these impurities facilitated the leaching of tungstic acid catalysts into the solution due to the formation of salts [55]. There are also examples of other acid heterogeneous

catalysts commonly employed in biomass hydrolysis, including commercial acid zeolites, Amberlysts, and acid-modified SBA-15, which exhibit deactivation under various reaction conditions [57–59]. Acid zeolites, for instance, are susceptible to deactivation when exposed to ions like K, Ca, and Mg in the feed solution. This occurs due to the ion exchange process, where these metal ions replace H^+ ions within the zeolitic microstructure, resulting in the loss of acidic properties and in a subsequent decline in the catalyst activity [59,60]. By contrast, some impurities have been reported to exhibit negligible or even sometimes positive effects on the hydrolysis of cellulose. In a study by Pang et al., it was observed that Na^+, K^+, and Cl^- ions remained inert during the conversion of cellulose under the tested hydrothermal conditions [55]. Additionally, Potvin et al. demonstrated that the addition of NaCl significantly enhanced the LA yield in the cellulose hydrolysis catalysed by Nafion SAC-13. They reported that the addition of the salt caused the beneficial interaction with the hydrogen bonding network of the cellulose. Simultaneously, the hydrothermal conditions of the reaction facilitated a higher cellulose dissolution in the solvent. This dual action allowed the Nafion catalyst to more effectively hydrolyse cellulose, generating glucose and subsequently leading to increased LA production [61].

Impurities such as Pb, Cd, and Zn are also identified to influence the hydrolysis reaction. Their presence can result in catalyst deactivation as the protons of the solid acid catalysts can be replaced by these metal ions [62,63]. The summary of the effects of the impurities during the hydrolysis step is shown in Figure 6.

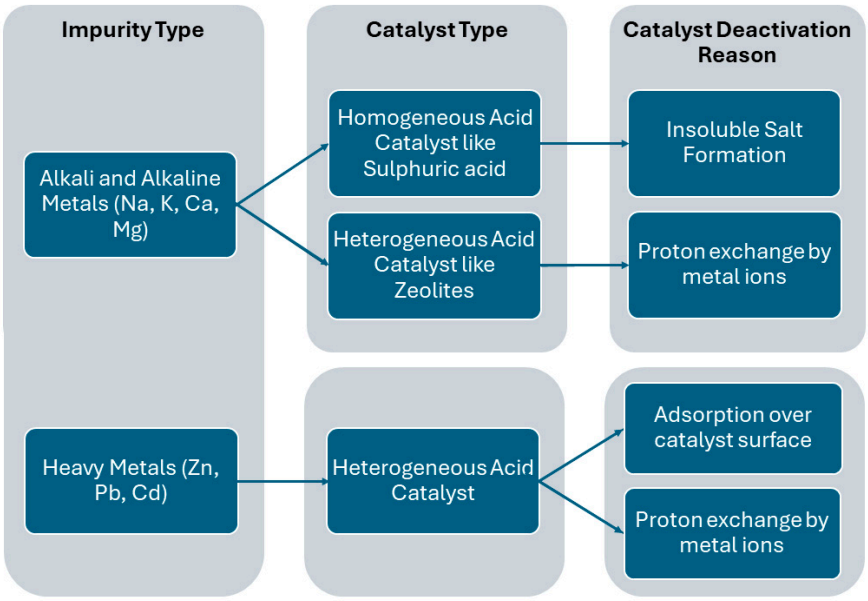

Figure 6. Catalyst deactivation during the hydrolysis step by endogenous types of impurities.

Impurities present in the biomass not only impact the hydrolysis process but also significantly affect the further hydrogenation reactions of the further upgrading of platform chemicals performed with metal-based catalysts.

Both noble and non-noble metals are used for this reaction efficiently, with the following included as typical examples of active phases: Ru, Pt, Pd, Ni, and Cu [9–11]. In general, the properties of catalysts can be influenced by presence of inorganic components through changes in how they adsorb the reactants. This deactivation can usually occur by either blocking the active surface sites, making them inaccessible for adsorbing molecules (geometric effects), or by inducing structural modifications due to strong interactions with metal impurities (electronic effects) [64,65].

By contrast to studies on the effect of impurities during the hydrolysis step, investigations concerning the hydrogenation step remain scarce. Indeed, in the case of the hydrogenation of LA derived from depithed sugarcane bagasse feedstock, Mthembu et al.

pointed out the possible presence of impurities in the LA substrate, but in their case, the loss in performance in the hydrogenation to GVL was relatively minor [66]. No information was provided on whether the potential impurities were originating from the depithed sugarcane bagasse feedstock itself, or from the chemical process chain.

Biogenic impurities like alkali and alkaline earth metals and heavy metals such as Pb, Cd, and Zn are identified to influence hydrogenation reactions. They are considered as potential impurities during biomass chemical processing since these inorganic salts can leach and in consequence can be released into the aqueous solution. Studies have indicated that inorganic impurities such as Zn and Pb can hinder the activity of Ru catalysts used during LA hydrogenation through adsorption on their surface. This phenomenon is likely attributed to the adsorption of contaminants at the Ru active sites, leading to the poisoning of the catalyst [42].

4.2. Impurities from Plant Proteins

Protein content has been reported to strongly differ depending on the plant species. Although protein contribution is the highest in aquatic plants, other species such as corn or sugarcane (particularly their leaves) contain also significant amounts of proteins [5]. Proteins are present in the form of photosynthetic pigment–protein complexes (PPCs) which can be notably found in the biomass leaves and which comprise a set of chromophore molecules, typically bacteriochlorophyll species, held in a well-defined arrangement by a protein scaffold (Figure 7). They are a vital component of the light-harvesting machinery of all plants, enabling the efficient transport of the energy of absorbed light towards the reaction centre, where chemical energy storage is initiated. Plant proteins are made up of about 20 common naturally occurring 'biogenic' amino acids identified within the biomass feedstock, among them aspartic acid, glutamic acid, leucine, proline, histidine, glycine, threonine, arginine, alanine, tyrosine, cysteine, valine, methionine, tryptophan, phenylalanine, isoleucine, lysine, and serine [67].

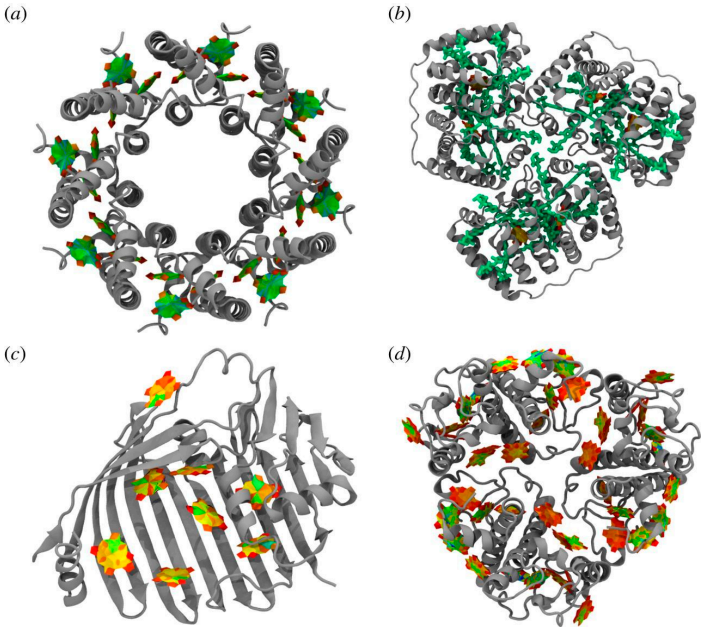

Figure 7. Crystal structures of four representative PPCs found in green plants: (**a**) *Rhodospirilum molischanum* (PDB: 1LGH), (**b**) *Amphidinium carterae* (PDB: 1PPR), (**c**) Fenna–Matthews–Olson (FMO) complex (PDB: 3EOJ), and (**d**) *Spinacia oleracea* (PDB: 4LCZ). In each case, the coloured parts of the PPC represent the chromophore molecules, with the rest of the protein shown in grey. Reproduced from ref [68] with the permission of The Royal Society.

Metal catalysts for hydrogenation are susceptible to deactivation by biogenic impurities [69]. In particular, biogenic amino acids that contain sulphur in their structure, such as

cysteine and methionine, have been reported to strongly impact the further conversion of biomass-derived substrates. For example, the effect of cysteine, alanine, and methionine amino acids was studied on the hydrogenation of LA using the Ru/ZrO_2 catalyst. It was found that cysteine and methionine (sulphur-containing amino acids) significantly inhibited catalytic activity in dioxane. In another study, researchers described that cysteine can be a potential source for metal sulphide formation during the hydrogenation of glucose and xylose – but under similar reaction conditions than for LA hydrogenation -, which causes the irreversible deactivation of a titania-supported Ru catalyst by poisoning the catalytic active sites by adsorption [40].

In contrast, alanine (non-sulphurous amino acid) was found to have no major impact on hydrogenation. However, even traces of cysteine deactivated the Ru/TiO_2 catalyst when hydrogenation was performed in water. The authors concluded that the deactivation was caused by the irreversible interaction between sulphur-containing amino acids and the Ru sites of the catalyst [40]. Ru poisoning by sulphur was also documented by Zhang et al. They investigated the influence of cysteine, alanine, and methionine amino acids on the hydrogenation of another carboxylic acid like lactic acid, which can be considered similar to LA [70]. Similar to the above study, they found that cysteine and methionine irreversibly deactivated the Ru/C catalyst due to the strong adsorption of sulphur on ruthenium active sites, thus poisoning the catalyst. Further, it was described that the sulphur-containing amino acids can partially fill the porous structure of the activated carbon and thus block lactic acid access to the catalyst (Ru/C). They reported the possibility of sulphur present in albumin in the form of cysteine and methionine, to directly poison the Ru surface by adsorption. Poisoning could be an issue especially if the protein unfolds in the carbon pore structure in the presence of hydrogen and at low solution pH. Therefore, a two-fold poisoning mechanism was proposed, with first the plugging of pores by the protein and second the poisoning of the metal active sites via the sulphur from the sulphur-containing amino acids. However, they observed that alanine caused a decrease in catalytic activity due to competitive adsorption, resulting from the preferential adsorption of alanine molecules on the metal surface over lactic acid [70].

4.3. Influence of Other Compounds

A series of molecules resulting from the hydrolysis step of the chemical processing of biomass have been identified as impurities potentially impacting the performances of the catalysts used in the LA hydrogenation reaction [40]. Those molecules are HMF and FFR, which are the main products of the C-6 and C-5 sugars hydrolysis, respectively, as well as FA, which is the by-product of C-6 sugar hydrolysis formed in equimolar amount with LA. Although the use of FA as an internal source of hydrogen is a very appealing step forward in the sustainable integration of biomass chemical processing within biorefineries, it requires efficient one-pot catalysis to drive both the selective decomposition of FA to hydrogen and the subsequent hydrogenation of LA into GVL. FA decomposition can proceed via two reaction pathways, namely by dehydrogenation with the formation of H_2 and CO_2 (1) and by dehydration with the formation of CO and H_2O (2).

$$HCOOH \rightarrow H_2 + CO_2 \quad (1)$$

$$HCOOH \rightarrow CO + H_2O \quad (2)$$

FA present in the reaction mixture can act as poison and deactivate metal-based catalysts by irreversible chemisorption of the molecule on the metal active sites. In our previous studies, we showed that ruthenium-based catalysts (Ru/C and Ru/TiO_2) are susceptible to poisoning by FA, which can block their active sites and hinder their catalytic activity. The first step in the hydrogenation of LA to GVL with FA as a hydrogen source is the breaking of the OH bond in formic acid. This step is also the slowest, requiring the highest activation energy (1.08 eV). When the OH bond is broken, it forms a formate intermediate on the Ru surface. However, this formate intermediate can poison the catalyst,

preventing further reaction [71]. Deng et al. found that even a very small amount of formate (10 mmol/L) can significantly inhibit the conversion of LA [44]. This results from the strong adsorption of the formate on Ru (0001), which blocks the active sites. The inhibition of the active sites by the surface formate species persists until a sufficiently high conversion of formic acid occurs, making free the catalytic sites for LA hydrogenation [42,71].

The co-produced CO and CO_2 during the FA decomposition also have detrimental effects on the activity of the catalysts. CO_2 under hydrogen pressure might also create surface formate species, which hinders the conversion of LA. As a result, the overall catalytic efficiency of Ru/C is greatly reduced when CO_2 is introduced into the reaction mixture. This highlights the complex relationship between surface species and catalytic reactions in this system [42,71]. Like the formate species, CO can also adsorb strongly on the catalyst surface, acting as a poison for the active metal centres (as explained above). We investigated the effect of CO using Ca-modified titania-supported Ru catalysts in our earlier work. It was observed that the catalyst preparation method, particularly the Ca modification, plays a pivotal role in determining the extent of FA decomposition and its subsequent impact. Catalysts modified with Ca exhibited improved the selectivity to H_2 during the FA decomposition, generating less CO compared to other catalysts; therefore, catalysts were poisoned to a lower extent. Furthermore, the incorporation of Ca^{2+} ions into the TiO_2 crystal lattice altered metal-support interactions, reducing CO adsorption [72].

In the bimetallic system Ni-Au, it was found that even traces of CO during the reaction exhibit a significant impact on catalytic performance. Investigations revealed that chemically reduced monometallic gold exhibited limited activity in FA decomposition. Conversely, Ni/γ-Al_2O_3, a catalyst incorporating chemically reduced nickel, demonstrated notable activity with a 52% FA conversion rate. The introduction of bimetallic Au-Ni/γ-Al_2O_3 catalysts further underscored the impact of CO, surpassing the monometallic counterparts and displaying the highest activity (91%) among catalysts prepared by chemical reduction. To comprehend the superior performance of the Au-Ni catalysts, the study employed density functional theory (DFT) calculations, specifically focusing on FA decomposition. The DFT analysis compared a model Au-Ni (111) surface with Au (111) and Ni (111), revealing insights into the catalytic mechanism. The dehydrogenation process commenced with OH scission, leading to the formation of a bidentate formate intermediate on all three surfaces. On the Au-Ni surface, this intermediate exhibited a strong Ni-O bond and a weak Au-O bond, influencing its stability and favouring the overall reaction. Weaker hydrogen adsorption on the alloy promoted hydrogen production. While CO could potentially poison active sites on monometallic surfaces like Ni (111), the alloying effect on Au-Ni surfaces reduced the number of Ni-CO bonds, weakening CO adsorption. Moreover, the alloy facilitated the reverse hydroxylation of CO into carboxyl (COOH), a competitive process with desorption. These COOH groups can be easily hydrogenated to regenerate formic acid when exposed to hydrogen, thereby minimizing the adverse effects of CO on catalytic sites. These findings highlighted that while CO formation during FA decomposition poses challenges for monometallic catalysts, strategic alloying in bimetallic Au-Ni catalysts serves to decrease CO-induced poisoning, thereby enhancing catalytic efficiency in LA conversion [73].

In another study, it is highlighted that Pd in the Ag-Pd bimetallic system, while active in catalysis, is prone to poisoning by CO. Computational studies on monometallic Ag and Pd surfaces, as well as bimetallic systems, emphasise that intermediates (formate) formed during the reaction have strong bonds with Pd sites, risking the potential poisoning of the catalyst. However, the bimetallic catalyst (4% Ag–1% Pd) showed superior performance due to strong Ag-Pd interactions, and the dilution of Pd in the Ag-based alloy was suggested to minimize the adsorption of CO due to the isolation of Pd atoms (i.e., one Pd atom surrounded by Ag), enhancing the efficiency of the catalyst [74].

Furthermore, the decomposition products of FA that are H_2, CO, and CO_2 can be responsible for other side reactions, such as methane formation, mainly through reactions (3) and (4).

$$CO + 3H_2 \rightarrow CH_4 + H_2O \quad (3)$$

$$CO_2 + 4H_2 \rightarrow CH_4 + 2H_2O \quad (4)$$

These methane-forming reactions compete with the desired LA hydrogenation reaction for hydrogen, thereby reducing the efficiency of LA hydrogenation [71]. The acidity of FA also promotes the formation of carbonaceous deposits (coke) on the catalyst surface by the condensation of reaction intermediates. These deposits block the active sites and hinder the ability of the catalysts to carry out the desired reaction. For instance, Ni-based catalysts (Ni/H-ZSM-5, Ni/SiO_2) showed gradual decreases in LA conversion and GVL yield over the time of reaction due to the FA-induced formation of coke [75,76].

On the other hand, competitive adsorption occurs when FA molecules or other compounds formed during biomass hydrolysis, such as furfural and HMF, adsorb onto the catalyst active sites. Using ultrafine Ru nanoparticles supported on lignin-derived N-doped carbon layers as catalyst, Guo et al. observed that an excessive FA/LA ratio resulted in significant reduction in both LA conversion and GVL yield, which decreased from 99.5% and 98.4% to ca. 39.2% and 34.6%, respectively. They proposed that this resulted from a loss in GVL selectivity and from the deactivation of the catalyst under high acid concentration [77].

It is reported that the catalytic activity of Ru/ZrO_2 and Ru/TiO_2 decreased because HMF and FFR were adsorbed on Ru sites [40]. This prevents the target molecules (FA and LA) from adsorbing at the catalyst surface, in consequence reducing the catalytic activity. Following a deep GC–MS analysis, Grillo et al. reported the presence of traces of byproducts generated by the biomass conversion with LA used as starting substrate for the production of GVL, namely acetic acid (0.5%), propanoic acid (0.7%), and additional unknown compounds (6.8%) [78].

The summary of the endogenous type of impurities and their effect on the hydrogenation step is presented in Figure 8.

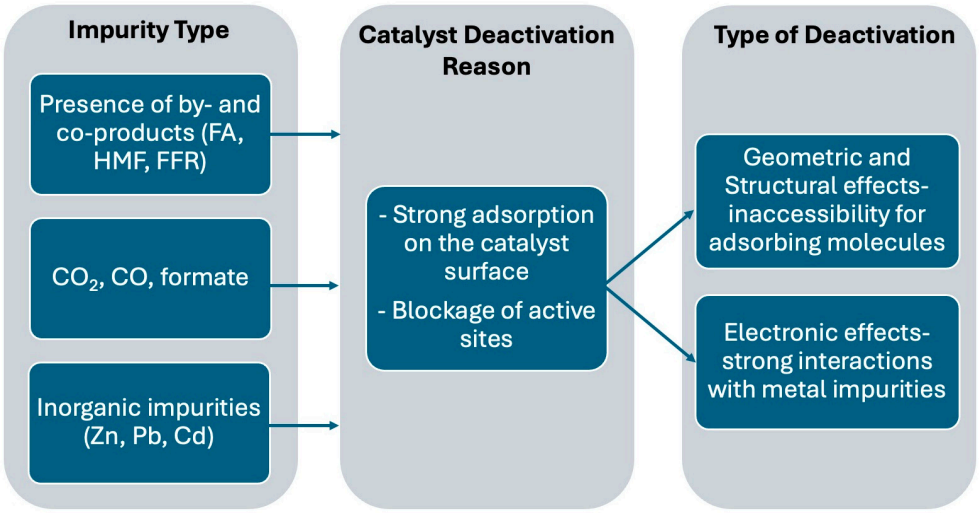

Figure 8. Catalyst deactivation during the hydrogenation step by endogenous type of impurities.

5. Biomass Exogenous Impurities

Exogenous impurities of biomass are mainly related to the presence of the catalysts used the initial hydrolysis step, to the application of physical pre-treatments to the raw biomass feedstock, and to the implementation of experimental reactor setups.

5.1. Influence of the Catalysts Originating from Hydrolysis Step

Ftouni et al. studied the influence of sulphuric acid (typical homogenous catalyst for biomass hydrolysis) as a feed impurity on the performance of Ru-based catalysts in the liquid phase hydrogenation of LA. Their findings highlighted the extreme sensitivity of Ru/C catalysts to minor amounts of H_2SO_4 (0.025–0.1 wt%), which inhibited the selective hydrogenation of LA to GVL due to the strong chemisorption of sulphur species on Ru active sites [38]. In a related study, Braden et al. demonstrated that the H_2SO_4 impurity adversely affected the activity of a Ru/C catalyst in LA hydrogenation in water, whereas a RuRe/C bimetallic catalyst exhibited lower activity but greater stability in the presence of the same impurity [39]. The stability of the RuRe/C catalyst was attributed to its bimetallic design, fostering synergistic effects between Ru and Re. The catalyst maintained intimate contact between Ru and Re under reducing conditions, as revealed by TPR studies, and XRD analysis confirmed the well-dispersed nature of Ru and Re species on the carbon support even after exposure to sulphuric acid. This structural integrity prevented agglomeration, contributing to the stability of the catalyst and to the efficiency of the LA hydrogenation, and in consequence making the catalyst resilient to the adverse effects of sulphuric acid impurities.

Additionally, Genuino et al. observed that Ru catalysts supported on ZrO_2 remained active in LA hydrogenation in dioxane even in the presence of H_2SO_4. The stability of Ru/ZrO_2 against deactivation was attributed to the sulphate ion adsorption capacity of the oxide support, essentially acting as a scavenger [38,40]. Similar findings were found for reactions conducted in water, where zirconia support allowed for higher stability in comparison to silica or alumina for Ru catalysts tested in the hydrogenation of pure LA in comparison to one obtained from cellulose hydrolysis containing sulphuric acid [41].

However, the situation changed when the catalyst testing was carried out in a continuous-flow reactor. It was also observed that the Ru/ZrO_2 catalyst exhibited superior stability in dioxane compared to its Ru/TiO_2 counterpart using reagent-grade LA as the substrate. The diminished stability of Ru/TiO_2 in dioxane was attributed primarily to the reduction of a significant fraction of TiO_2 support, wherein Ti^{4+} species were reduced to Ti^{3+}. By contrast, both catalysts were found stable in water, with minimal deactivation. The influence on the GVL productivity of the H_2SO_4 concentration added to the feed (0.1 to 1 wt%) was also explored. It was noted that increasing the H_2SO_4 amount from 0.1 to 0.25 wt% led to a slight decrease in GVL yield by up to 5% while maintaining full selectivity to GVL. However, when the H_2SO_4 content reached 0.5 wt%, a noticeable reduction in GVL yield to 55% occurred, indicating a maximum sensitivity threshold for the Ru/ZrO_2 catalyst. Adding an H_2SO_4 concentration of 1.0 wt% resulted in the nearly complete inhibition of the catalyst activity, leading to very low LA conversion and GVL yields. The presence of H_2SO_4 led to the irreversible deactivation of both catalysts, as sulphur poisoning occurred, adversely affecting the active Ru sites.

Sulphur-containing impurities, known for their strong adsorption on metal surfaces, hindered the adsorption of the reactant molecules, resulting in a substantial loss of catalytic activity [38,43,79]. The specific impact of sulphur-containing impurities on the Ru-based catalysts was found to depend on both the oxidation and the protonation state of the sulphur-containing potential poison, as well as on its easy reduction under the reductive conditions. Previous studies revealed that under reductive and acidic conditions, surface sulphates could be reduced to sulphides, contributing to the formation of Ru sulphides and sulphates, and ultimately leading to the poisoning of the active Ru surface [80,81]. Similarly, Molder et al. found that S- and N-containing components were the root cause of the deactivation of heterogeneous Raney Ni catalysts in the hydrogenolysis of herbaceous biomass (hay). Sulphur-containing components were particularly more poisonous than nitrogen-containing ones [82].

5.2. Physical Pre-Treatments

Biomass valorisation often involves physical pre-treatments to disrupt the complex structure of biomass and enhance its accessibility to subsequent processes. Ball milling is one of the most popular mechanical pre-treatments and is a mechanical method that breaks the polymer biomass by grinding it into smaller particles [83]. While ball milling is widely used due to its simplicity and high energy efficiency, it can introduce contaminants that can negatively impact the downstream conversion processes, including the conversion of LA. Ball milling can introduce impurities into biomass in several ways. The mechanical forces generated during the ball milling can break down biomass components into smaller fragments, leading to the release of lignin fragments, hemicellulose degradation products, and even cellulose chain breakage. These byproducts can act as inhibitors; for example, lignin fragments can be the source of carbon deposits, hence negatively impacting further conversion processes. Mayer-Laigle et al. pointed out that the contamination of biomass materials by the grinder or milling media is a significant factor to consider when selecting the milling equipment. In their study of wheat straw milling, they highlighted that ball milling can contaminate the biomass, as it led to the formation of a fine powder of biomass compounds with enhanced abrasion and adhesion phenomena with the milling balls. Abrasion can introduce metal impurities into biomass as ball mills often contain steel or other metallic components that can break off and contaminate the biomass, while adhesion can form clumps of biomass that are difficult to break down further [84]. In another study, Di Nardo and Moores examined the impact of the milling jar and ball material on the contamination of chitin polysaccharides during mechanochemical amorphization. They investigated the extent of contamination caused by different milling media, namely stainless steel (Fe), zirconia (Zr), brass (Cu), aluminum (Al), and tungsten carbide (W). Their findings revealed that zirconia yielded minimal contamination, while all other metal-containing systems produced significantly higher levels of contamination. The metal leaching from the reactors followed the order Fe < W < Al < Cu. This was attributed to metal release during milling, presumably coming from friction and scratching between the grinding balls, the powdered material, and the milling vessel [85].

5.3. Experimental Reactor Setup

The hydrolysis of biomass is a crucial step in the production of bio-based products. This process typically involves the use of acidic catalysts, such as hydrochloric acid or sulfuric acid, to break down the complex carbohydrates in biomass into simpler sugars. However, the acidic media employed in hydrolysis pose a significant challenge, as they can lead to the leaching of metals from the reactor walls (particularly those made of stainless steel) into the reaction medium. The metals that are most susceptible to leaching from stainless steel are Fe and Cr. This leaching can have a detrimental effect on the catalytic activity and selectivity of downstream hydrogenation processes. A study by Arena et al. investigated the hydrogenation of glucose using a Ru/Al_2O_3 catalyst in a continuous-flow reactor made of stainless steel. Post-reaction analysis revealed the presence of iron within the reactor. The extent of iron buildup was directly correlated with the Ru content of the catalyst, meaning that the Fe concentration was increased with the Ru content. This suggests that iron is selectively adsorbed onto ruthenium sites, effectively blocking active sites, and reducing the activity of the catalyst. Subsequent analyses using atomic absorption spectrometry confirmed that the iron originated from the reactor walls [81,86]. Similarly, Kusserow et al. found that a Ru-based catalyst was deactivated by the leaching of chromium and silicon from a stainless steel reactor. XRF analysis of spent catalysts revealed indeed the presence of increased amounts of chromium and silicon interfering with the catalytic activity [87].

6. Catalyst Deactivation by Carbonaceous Species (Humins and Coke)

6.1. Catalysts Deactivation by Humins

Humins are heterogeneous, complex organic solids that are formed as byproducts during various thermochemical conversion processes of biomass, including hydrothermal conversion, pyrolysis, and gasification. Their amorphous, carbonaceous nature and not-defined structure pose significant challenges in biomass valorisation efforts [88,89]. The formation of humins is predominantly attributed to acid-catalysed biomass hydrolysis. During this process, cellulose, the primary component of biomass, undergoes depolymerisation, yielding glucose and other degradation products like acetic acid and HMF. These intermediate compounds can further react under acidic conditions, leading to the formation of humins. The exact mechanism underlying the formation of humins remains ambiguous, but it is believed to involve condensation reactions and the polymerisation of intermediate compounds. Lignin, another major component of biomass, plays a crucial role in the formation of humins. While lignin remains largely insoluble in acidic conditions, its presence facilitates the formation of humins by providing a reactive surface for condensation reactions [90,91]. This, in turn, can lead to reduced yields to the desirable products such as LA and FA, especially over an extended reaction time. The presence of humins can significantly hinder the production of LA and FA in several ways (Figure 9). First, humins exhibit a strong affinity for LA and FA, leading to their adsorption onto the humin surface. This reduces the availability of LA and FA for further conversion or downstream processing. Second, humins can deposit onto the surface of catalysts, particularly around the active sites, effectively blocking access to LA molecules. This deactivation of catalysts can significantly reduce their effectiveness in promoting LA and FA production. What is more, humins can aggregate and form larger particles that can clog the pores of catalysts, further hindering the diffusion of reactants and products. This further reduces the catalytic activity and the overall efficiency of the conversion process [62].

Using directly carbohydrate-rich biomass waste as feedstock, Koranchalil and Nielsen have associated the formation of insoluble humins to the diminished activity and the low yields to GVL obtained using the homogeneous Ru-MACHO-BH catalysts in aqueous H_3PO_4, which are favoured under higher H_3PO_4 acid concentration and higher temperature [92]. They speculate that humins are formed to a greater extent in the more concentrated samples [93].

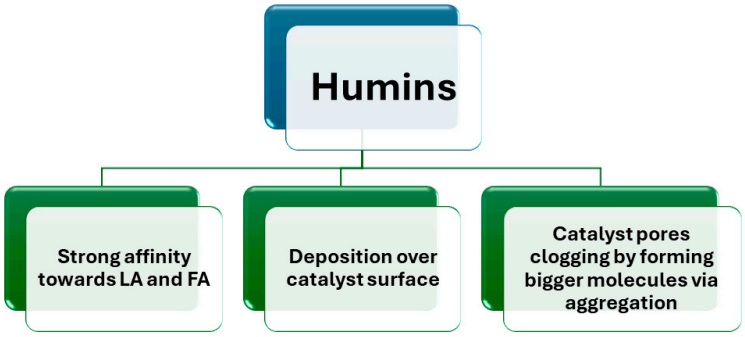

Figure 9. Different influence of humins on GVL production.

Several studies have investigated the effects of humins on GVL production from LA or cellulosic feedstock. For example, a study comparing the one-pot cellulose hydrolysis followed by hydrogenation in separate reactions revealed that the former method resulted in significantly lower GVL yields due to increased carbonaceous species formation, particularly humins, which effectively deactivated the used ruthenium catalyst (Ru/TiO_2). The time-of-flight secondary ion mass spectrometry (ToF-SIMS) analysis of spent catalysts confirmed the presence of higher carbonaceous deposits in the one-pot reaction, indicating excessive humin generation. This accumulation of carbonaceous species, primarily coming from humins, effectively hindered the GVL production efficiency, leading to a drastic

reduction in yield from 31% to 6% [43]. Another study found that Ru/ZrO_2 and Ru/TiO_2 catalysts were reversibly deactivated by humins during the hydrogenation of LA to GVL. This was attributed to the fact that humins are rich in carbonyl functional groups and furan rings (furfural and HMF), which can adsorb onto the catalyst surface and block active sites [40].

Cellulose hydrolysis was also hampered by humins formation in pure water when Amberlyst 70 was used as an acid catalyst, resulting in a low yield to LA (20%). However, the yield was significantly increased to 69% when a solvent mixture of 90% GVL and 10% water was utilized. This is attributed to the ability of GVL to solubilise cellulose and humins in the presence of acid catalysts [94]. GVL facilitates the interaction between the cellulose and the solid acid catalyst, enabling the production of LA under mild conditions. Therefore, GVL effectively converts cellulose into soluble products and prevents the precipitation of humins. Notably, high LA yields (54%) were also obtained when using real biomass (corn stover), demonstrating the versatility and effectiveness of this method [95]. Moreover, when FA was used as a catalyst for the dehydration of fructose to LA, the conversion was full, but only half of the fructose was converted to LA, the remaining half being transformed into undesirable solid compounds (humins). As catalyst deactivation by humins could be reversible, the approach of calcining the used catalyst (500 °C for 4 h) was implemented by the Ebitani group to remove poisoning humins by combustion from the catalyst surface in the case of Au/ZrO_2 and Ru/SBA-15 catalysts used in the one-pot dehydration/hydrogenation of fructose to GVL [96]. While the approach was not successful on the Ru/SBA-15 catalyst (only 9% GVL yield being obtained for the 3rd run), the Au/ZrO_2 catalyst was capable of retaining a significant fraction of its initial activity with a gradual decrease in GVL yield from 48 to 37% during recyclability tests.

6.2. Catalysts Deactivation by Coke

Furthermore, humins are considered to be precursors of coke. Through a combination of reactions, including aldol condensation, nucleophilic addition, and electrophilic addition, humins polymerise into oligomers. These oligomers further crosslink to create a complex network that deposits onto catalysts as a carbon deposit, forming a dense layer of coke [93,97]. There are two main mechanisms of carbon deposition, namely fouling and coke formation. Fouling is the physical adsorption of species from the liquid phase onto the catalyst surface, which can block active sites or pores and lead to activity loss. Coke formation is the chemisorption of hydrocarbons or carbon species that decompose or condense on the catalyst surface. Coke formation is catalysed by acid sites, and cyclisation and dehydrogenation reactions on acid sites can lead to the formation of aromatic compounds that can further react to form heavy hydrocarbons that can condense and polymerise as coke [98]. Coke can adsorb as a monolayer or multilayer and block the access of substrates to metal active sites, encapsulate metal particles, and completely deactivate them, or plug micro- and mesopores and block the access of substrates to metal crystallites [98]. Coke can take many forms depending on the conditions under which it is formed, and its chemical structure can vary greatly depending on the reaction conditions, the catalyst, and the type of reaction [99].

In the case of LA hydrogenation, the acidic hydrothermal conditions can easily lead to the formation of coke, which is believed to be caused by the condensation of intermediates like angelica lactone (AL) during the conversion of LA [100,101]. Coke deposition results in a rapid decrease in GVL selectivity and accelerated catalyst deactivation. The acidic conditions are considered as the main factor responsible for coke formation [102–104]. Putro et al. observed a gradual decrease in catalytic activity for the conversion of LA over Pt/TiO_2 and acid-activated bentonite as a co-catalyst after consecutive reaction cycles. The co-catalyst was found to promote GVL opening via ALs, which were polymerising further to form coke deposits [105]. Similarly, the $Co/\gamma\text{-}Al_2O_3$ catalyst was deactivated due to coke formation over the catalytic active sites by ALs. It was observed that the accumulation of coke on the catalyst surface reduces its activity by diminishing the number

of active sites available for hydrogenation. However, the addition of Ni to Co/γ-Al_2O_3 improved the activity of the catalyst and its resistance to coke formation. The rate of carbon deposition on the catalysts was found to be directly correlated to the yield to GVL. The Ni-Co/γ-Al_2O_3 catalyst was shown to maintain its activity in converting LA to GVL with a lower carbon deposition rate than the Co/γ-Al_2O_3 catalyst, i.e., 0.43 mmol·gcat^{-1}·h vs. 1.014 mmol·gcat^{-1}·h^{-1}, demonstrating the significant beneficial influence of Ni within the bimetallic catalyst [106]. The improved catalytic activity of the bimetallic catalyst was ascribed to the increase in the active metal surface area and the presence of smaller active metal particles induced by the addition of Ni to Co/γ-Al_2O_3, in comparison to the monometallic Co catalyst.

Coke deposition is particularly pronounced on Ru-based catalysts supported on strongly acidic zeolites (H-ZSM5 and H-β) compared to those supported on non-acidic supports (Nb_2O_5 and TiO_2, ZrO_2) [40,107]. This difference is attributed to the stronger Brønsted acidity of zeolites, which promotes the polymerisation of carbonaceous species. The TGA analysis of spent Ru catalysts supported on different materials revealed that the deactivation trend (based on the weight loss) followed the order: H-ZSM5 > H-β > Nb_2O_5 > TiO_2 [40,108]. Coke deposition not only reduces the number of active sites but also affects other catalyst properties such as the surface area and the pore volume. For example, Cao et al. described the deactivation of the Ru/C catalyst in LA hydrogenation in the strongly acidic media (pH = 1). They observed a huge drop in the surface area caused by the higher formation of carbonaceous species in the more acidic media [109]. Wettstein et al.'s study on carbon-supported Ru-catalysts for LA hydrogenation in a 2-sec-butyl-phenol (SBP) solvent further illustrates the detrimental effects of coke deposition. The monometallic Ru catalyst (Ru/C) exhibited the highest activity, hydrogenating both LA and SBP. However, its activity diminished over time due to coking. Incorporating Sn led to the formation of bimetallic Ru–Sn alloys, such as Ru_2Sn_3 and Ru_3Sn_7. These alloys displayed lower turnover frequencies for hydrogenation reactions compared to the monometallic Ru phase but exhibited improved catalyst selectivity and stability. Physisorption measurements confirmed the coking-induced decrease in surface area and pore volume for the Ru catalyst [110]. Another factor stimulating the coke deposit formation can be the higher reaction temperature, which was considered as an important factor diminishing the reaction selectivity for Pd catalysts [111].

Testing activated carbon and titania supported Ru catalysts, Grillo et al. proposed the explanation that humins remaining from previous conversion processing steps might cause the fouling of the catalyst surface by deposition or coke formation, to explain the strong influence of impurities on the conversion of LA directly derived from biomass, while selectivity was not impacted and remained complete [78].

There are also multiple examples of deactivation of many other systems like Mg-Al hydrotalcite catalysts and Cu- and Co-based catalysts by the reduction of the active site surface area or pore volume [112–114]. For instance, in addition to the sintering of Cu nanoparticles, Boddula et al. pointed out the role of coke deposits on active sites in the loss of activity in LA hydrogenation with time-on-stream observed on a 5 wt% Cu/SiO_2 catalyst at 265 °C after 20 h of reaction [113].

Fortunately, often the combination of calcination and subsequent reduction treatment has been demonstrated as an effective method for regenerating spent catalysts [105,115–117].

7. Summary

This review explores the effects of various impurities found in biomass on the hydrolysis of cellulosic feedstock to LA followed by its hydrogenation to GVL—Figure 10. Impurities are classified into two groups, namely endogenous and exogenous. Endogenous impurities include heavy metals like Zn, Pb, Cd, alkali metals (Na, K), alkaline earth metals (Ca, Mg), and sulphur from plant proteins. The composition of these impurities varies depending on the type of biomass (soft or hardwood), cultivation conditions, geographic location, climate, and harvesting techniques. Exogenous impurities, on the other hand, are

introduced from the reaction setup used during the physical pre-treatments or previous reaction steps (e.g., hydrolysis of cellulose).

In particular, ball milling equipment can introduce exogenous impurities like Fe, Cu, and Al into the biomass, while the reaction media can become contaminated with Fe and Cr from stainless steel reactors. These impurities can significantly affect both the hydrolysis and hydrogenation steps of the conversion process. Hydrolysis is typically carried out using homogeneous acid catalysts such as sulphuric acid and hydrochloric acid, which can stimulate leaching of metallic impurities into the aqueous solution.

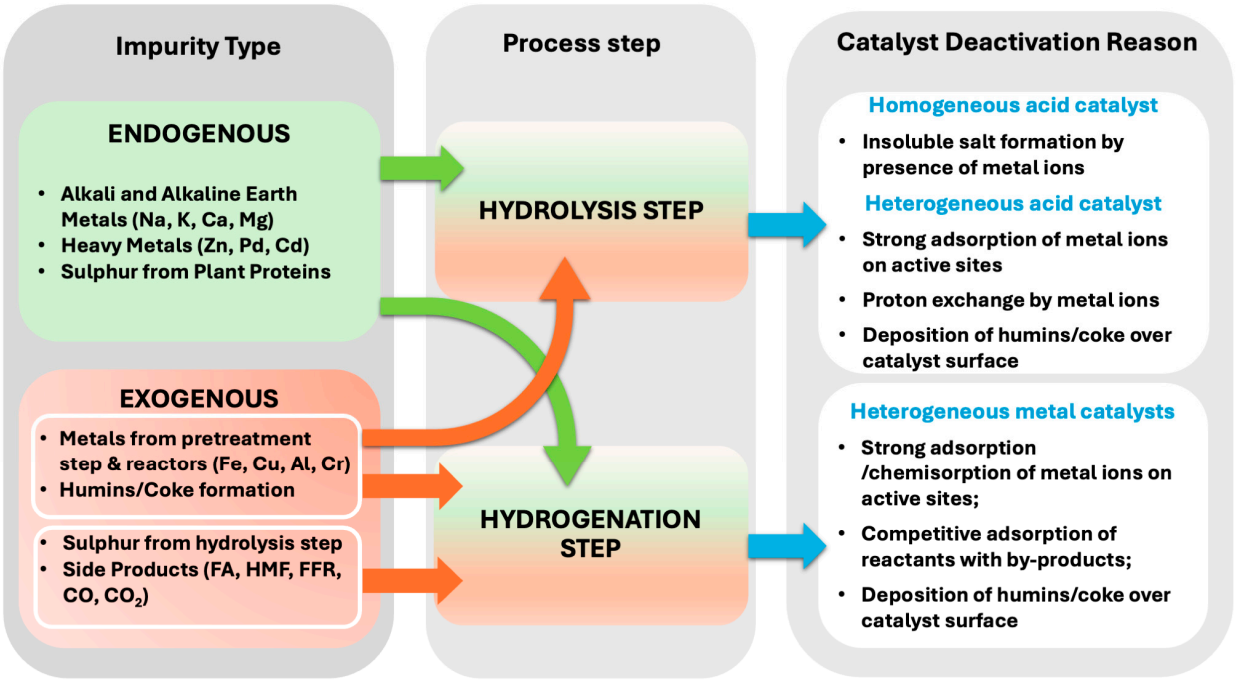

Figure 10. Impurities present in biomass and their effects on the catalyst deactivation during hydrolysis and hydrogenation steps.

Among endogenous impurities, calcium ions are particularly detrimental, as they readily form insoluble calcium sulphate even at low acid concentrations (0.005–1 M), hindering the hydrolysis reaction. Iron ions, on the other hand, can exhibit both positive and negative effects, while sodium ions, in contrast, have been found to have either no effect or even a beneficial effect on cellulose hydrolysis. In addition to homogeneous catalysts, heterogeneous acid catalysts like commercial acid zeolites, Amberlysts, and acid-modified SBA-15 are also used in biomass hydrolysis. However, they are susceptible to deactivation when exposed to ions like K, Ca, and Mg in the feed solution. For instance, zeolites can be deactivated by an ion exchange process where the metal ions replace H^+ ions of the zeolitic microstructure, leading to a loss of acidic properties and a subsequent decline in the catalytic activity.

Furthermore, inorganic impurities and byproducts such as FFR, HMF, and FA formed during hydrolysis can significantly impact LA hydrogenation to GVL. These impurities can either directly block active metal sites or indirectly affect the catalyst's ability to adsorb reactants by inducing structural changes due to strong interactions with impurities. Specifically, sulphur-containing impurities, such as sulphuric acid or sulphur from biogenic amino acids, can irreversibly chemisorb onto metal active sites, effectively diminishing the catalytic activity. Similarly, heavy metals like Zn, Pb, and Cd and the metal ions leached either from the reactor walls or from milling balls and jars can physically block the active sites by adsorption, making the catalyst inactive. On the other side, FA can directly poison the catalyst by strongly binding to the metal sites, while FFR and HMF can compete for active sites, reducing the accessibility of LA and FA to the catalyst. Additionally,

these byproducts can decompose or undergo further reactions, generating methane and carbonaceous deposits, such as humins and coke, on the catalyst surface. Humins can irreversibly adsorb onto the catalyst, while coke can form a solid layer, further hindering the catalytic performance.

Additionally, although this was not the main aspect of the review, it should be noted that great care should be taken to avoid the presence of impurities resulting directly from the synthesis of the catalysts. For instance, Zhao et al. showed that the performances of acid−base amphoteric amorphous $Zr(OH)_4$ catalyst in the catalytic transfer hydrogenation of liquid-phase LA to GVL were impacted by the presence of Si and the formation of new Zr-O-Ti sites in the catalyst, which resulted from an inevitable dissolution of silicon species from glassware [118].

8. Future Perspectives

In considering future perspectives dealing with the effect of impurities on the biomass conversion, it is crucial to address challenges caused by various impurities. In order to avoid impurities from biomass in the initial step, strategies should be explored to optimize biomass pre-treatments. For example, real-time monitoring and control can be utilized to detect the presence of impurities and in consequence to adjust the reaction conditions accordingly.

Understanding the impact of physical pre-treatment methods, such as ball milling, on the impurity introduction and developing methods to minimize contamination would contribute to cleaner biomass conversion processes. Furthermore, advances in biomass hydrolysis processes, particularly through the use of less acidic or alternative catalysts such as acidic ionic liquids $[C_4H_8SO_3Hmim][HSO_4]$, hold the potential to mitigate the leaching of metals from the reactor walls and thus the associated catalyst deactivation.

The detrimental effects of impurities on LA hydrogenation can be minimized by implementing strategic approaches. One approach could be the development of robust catalysts with enhanced resistance to impurities. This may involve exploring novel catalyst materials or modifications that mitigate poisoning effects and can thus sustain catalytic activity during LA hydrogenation. Another feasible strategy is to comprehensively understand the mechanisms by which the impurities poison catalysts, providing insights for the development of more effective catalysts.

Further investigations into bimetallic systems, such as the Ru-Re and Au-Ni catalysts, and their ability to minimize the impact of impurities on the catalytic efficiency could provide valuable insights. Introducing a second metal can enhance the metal dispersion, prevent the agglomeration, and contribute to the stability and the effectiveness of the catalyst. Additionally, metal doping can influence the particle size, the metal-supported interactions, and the adsorption strength, resulting in improved catalytic activity and selectivity. The issue of humins and coke formation can be addressed by gaining a comprehensive understanding of their formation mechanisms and developing catalysts that strongly resist their formation. Alternatively, strategies for effectively removing coke during the reaction can be explored. Investigating alternative reaction conditions or solvents, as demonstrated with GVL, may help to minimize the coke deposition and to extend the catalyst lifespan. Additionally, in-situ monitoring of the catalyst deactivation and exploring the regeneration potential of spent catalysts could pave the way for a sustainable and efficient biomass conversion into valuable chemical products, such as LA followed downstream by GVL.

Beside works on specific steps of the process chain transforming biomass, future works should first include the realization of more case studies starting from real biomass feedstocks and investigating stepwise the impact of both endogenous and exogeneous types of impurities present or introduced in the overall process chain of biomass operating from waste resource till the synthesis of the high added value compounds. Second, subsequent to the lab-scale investigations, upscaling studies need also to be encourage involving the implementation of the process chain applied to the real biomass feedstock at the (semi)-pilot

plant level in order to get data of strategical importance for the industrial actors involved. Third, the strategies followed for minimizing the presence of the impact of impurities should also be evaluated in terms of cost-effectiveness and scalability in industrial settings, and not only in terms of pure scientific aspects. Research on those aspects remains still in its infancy.

So, we hope that our review will serve to inspire the cross-fertilization of ideas and new projects involving academic and industrial cooperation in the yet under-investigated field of research devoted to the impact of endogenous or exogeneous impurities, to the base integration of mitigation strategies in the development of efficient catalysts and processes, as well as to the upscaling of both materials and processes.

Author Contributions: Conceptualization, N.K. and A.M.R.; methodology, N.K. and A.M.R.; investigation, P.K., M.B., N.K. and A.M.R.; resources, N.K. and A.M.R.; writing—original draft preparation, P.K., M.B., N.K. and A.M.R.; writing—review and editing, P.K., N.K. and A.M.R.; visualization, P.K.; supervision, N.K. and A.M.R.; project administration, A.M.R.; funding acquisition, N.K. and A.M.R. All authors have read and agreed to the published version of the manuscript.

Funding: This research was partially funded by the National Agency for Academic Exchange (NAWA), grant number PPI/STE/2020/1/00027/U/00001.

Data Availability Statement: No new data were created.

Acknowledgments: P.K. acknowledges the project of the National Agency for Academic Exchange (NAWA) within the framework of the "STER" Programme—Internationalisation of Doctoral Schools" as part of the project "Curriculum for advanced doctoral education & training—CADET Academy of Lodz University of Technology" for financial support.

Conflicts of Interest: The authors declare no conflicts of interest.

References

1. Zhou, C.H.; Xia, X.; Lin, C.X.; Tong, D.S.; Beltramini, J. Catalytic Conversion of Lignocellulosic Biomass to Fine Chemicals and Fuels. *Chem. Soc. Rev.* **2011**, *40*, 5588–5617. [CrossRef]
2. Ruppert, A.M.; Weinberg, K.; Palkovits, R. Hydrogenolysis Goes Bio: From Carbohydrates and Sugar Alcohols to Platform Chemicals. *Angew. Chem.—Int. Ed.* **2012**, *51*, 2564–2601. [CrossRef]
3. Harmsen, P.F.; Huijgen, W.; Bermudez, L.; Bakker, R. *Literature Review of Physical and Chemical Pretreatment Processes for Lignocellulosic Biomass*; Food & Biobased Research: Wageningen, The Netherlands, 2010; Volume 28, ISBN 9789085857570.
4. Tursi, A. A Review on Biomass: Importance, Chemistry, Classification, and Conversion. *Biofuel Res. J.* **2019**, *6*, 962–979. [CrossRef]
5. Rabemanolontsoa, H.; Saka, S. Comparative Study on Chemical Composition of Various Biomass Species. *RSC Adv.* **2013**, *3*, 3946–3956. [CrossRef]
6. Jędrzejczyk, M.; Soszka, E.; Czapnik, M.; Ruppert, A.M.; Grams, J. *Physical and Chemical Pretreatment of Lignocellulosic Biomass*; Elsevier: Amsterdam, The Netherlands, 2019; ISBN 9780128151624.
7. Vassilev, S.V.; Baxter, D.; Andersen, L.K.; Vassileva, C.G. An Overview of the Chemical Composition of Biomass. *Fuel* **2010**, *89*, 913–933. [CrossRef]
8. Lin, Y.C.; Huber, G.W. The Critical Role of Heterogeneous Catalysis in Lignocellulosic Biomass Conversion. *Energy Environ. Sci.* **2009**, *2*, 68–80. [CrossRef]
9. Soszka, E.; Reijneveld, H.M.; Jędrzejczyk, M.; Rzeźnicka, I.; Grams, J.; Ruppert, A.M. Chlorine Influence on Palladium Doped Nickel Catalysts in Levulinic Acid Hydrogenation with Formic Acid as Hydrogen Source. *ACS Sustain. Chem. Eng.* **2018**, *6*, 14607–14613. [CrossRef]
10. Michel, C.; Zaffran, J.; Ruppert, A.M.; Matras-Michalska, J.; Jędrzejczyk, M.; Grams, J.; Sautet, P. Role of Water in Metal Catalyst Performance for Ketone Hydrogenation: A Joint Experimental and Theoretical Study on Levulinic Acid Conversion into Gamma-Valerolactone. *Chem. Commun.* **2014**, *50*, 12450–12453. [CrossRef] [PubMed]
11. Ruppert, A.M.; Agulhon, P.; Grams, J.; Wachala, M.; Wojciechowska, J.; Swierczynski, D.; Cacciaguerra, T.; Tanchoux, N.; Quignard, F. Synthesis of TiO_2-ZrO_2 Mixed Oxides via the Alginate Route: Application in the Ru Catalytic Hydrogenation of Levulinic Acid to Gamma-Valerolactone. *Energies* **2019**, *12*, 4706. [CrossRef]
12. Alonso, D.M.; Bond, J.Q.; Dumesic, J.A. Catalytic Conversion of Biomass to Biofuels. *Green Chem.* **2010**, *12*, 1493–1513. [CrossRef]
13. Li, X.; Xu, R.; Yang, J.; Nie, S.; Liu, D.; Liu, Y.; Si, C. Production of 5-Hydroxymethylfurfural and Levulinic Acid from Lignocellulosic Biomass and Catalytic Upgradation. *Ind. Crops Prod.* **2019**, *130*, 184–197. [CrossRef]
14. Li, M.; Cao, S.; Meng, X.; Studer, M.; Wyman, C.E.; Ragauskas, A.J.; Pu, Y. The Effect of Liquid Hot Water Pretreatment on the Chemical-Structural Alteration and the Reduced Recalcitrance in Poplar. *Biotechnol. Biofuels* **2017**, *10*, 237. [CrossRef]

15. Ahorsu, R.; Cintorrino, G.; Medina, F.; Constantí, M. Microwave Processes: A Viable Technology for Obtaining Xylose from Walnut Shell to Produce Lactic Acid by Bacillus Coagulans. *J. Clean. Prod.* **2019**, *231*, 1171–1181. [CrossRef]
16. Li, P.; Cai, D.; Luo, Z.; Qin, P.; Chen, C.; Wang, Y.; Zhang, C.; Wang, Z.; Tan, T. Effect of Acid Pretreatment on Different Parts of Corn Stalk for Second Generation Ethanol Production. *Bioresour. Technol.* **2016**, *206*, 86–92. [CrossRef] [PubMed]
17. Santos, C.C.; de Souza, W.; Sant Anna, C.; Brienzo, M. Elephant Grass Leaves Have Lower Recalcitrance to Acid Pretreatment than Stems, with Higher Potential for Ethanol Production. *Ind. Crops Prod.* **2018**, *111*, 193–200. [CrossRef]
18. Grande, P.M.; Viell, J.; Theyssen, N.; Marquardt, W.; Domínguez De María, P.; Leitner, W. Fractionation of Lignocellulosic Biomass Using the OrganoCat Process. *Green Chem.* **2015**, *17*, 3533–3539. [CrossRef]
19. Yuan, Z.; Wen, Y.; Kapu, N.S. Ethanol Production from Bamboo Using Mild Alkaline Pre-Extraction Followed by Alkaline Hydrogen Peroxide Pretreatment. *Bioresour. Technol.* **2018**, *247*, 242–249. [CrossRef] [PubMed]
20. Zheng, Q.; Zhou, T.; Wang, Y.; Cao, X.; Wu, S.; Zhao, M.; Wang, H.; Xu, M.; Zheng, B.; Zheng, J.; et al. Pretreatment of Wheat Straw Leads to Structural Changes and Improved Enzymatic Hydrolysis. *Sci. Rep.* **2018**, *8*, 1321. [CrossRef] [PubMed]
21. Hendriks, A.T.W.M.; Zeeman, G. Pretreatments to Enhance the Digestibility of Lignocellulosic Biomass. *Bioresour. Technol.* **2009**, *100*, 10–18. [CrossRef] [PubMed]
22. Sewsynker-Sukai, Y.; Naomi David, A.; Gueguim Kana, E.B. Recent Developments in the Application of Kraft Pulping Alkaline Chemicals for Lignocellulosic Pretreatment: Potential Beneficiation of Green Liquor Dregs Waste. *Bioresour. Technol.* **2020**, *306*, 123225. [CrossRef]
23. Xu, J.; Zhang, B.; Lu, X.; Zhou, Y.; Fang, J.; Li, Y.; Zhang, S. Nanoscale Observation of Microfibril Swelling and Dissolution in Ionic Liquids. *ACS Sustain. Chem. Eng.* **2018**, *6*, 909–917. [CrossRef]
24. Yoo, C.G.; Pu, Y.; Ragauskas, A.J. Ionic Liquids: Promising Green Solvents for Lignocellulosic Biomass Utilization. *Curr. Opin. Green Sustain. Chem.* **2017**, *5*, 5–11. [CrossRef]
25. Prado, C.A.; Antunes, F.A.F.; Rocha, T.M.; Sánchez-Muñoz, S.; Barbosa, F.G.; Terán-Hilares, R.; Cruz-Santos, M.M.; Arruda, G.L.; da Silva, S.S.; Santos, J.C. A Review on Recent Developments in Hydrodynamic Cavitation and Advanced Oxidative Processes for Pretreatment of Lignocellulosic Materials. *Bioresour. Technol.* **2022**, *345*, 126458. [CrossRef] [PubMed]
26. Paudel, S.R.; Banjara, S.P.; Choi, O.K.; Park, K.Y.; Kim, Y.M.; Lee, J.W. Pretreatment of Agricultural Biomass for Anaerobic Digestion: Current State and Challenges. *Bioresour. Technol.* **2017**, *245*, 1194–1205. [CrossRef] [PubMed]
27. Nair, L.G.; Agrawal, K.; Verma, P. Organosolv Pretreatment: An in-Depth Purview of Mechanics of the System. *Bioresour. Bioprocess.* **2023**, *10*, 50. [CrossRef]
28. Hoang, A.T.; Nguyen, X.P.; Duong, X.Q.; Ağbulut, Ü.; Len, C.; Nguyen, P.Q.P.; Kchaou, M.; Chen, W.H. Steam Explosion as Sustainable Biomass Pretreatment Technique for Biofuel Production: Characteristics and Challenges. *Bioresour. Technol.* **2023**, *385*, 129398. [CrossRef]
29. Shah, A.A.; Seehar, T.H.; Sharma, K.; Toor, S.S. Biomass Pretreatment Technologies. In *Hydrocarbon Biorefinery—Sustainable Processing of Biomass for Hydrocarbon Biofuels*; Elsevier: Amsterdam, The Netherlands, 2022; pp. 203–228. [CrossRef]
30. Rackemann, D.W.; Doherty, W.O.S. The Conversion of Lignocellulosics to Levulinic Acid. *Biofuels Bioprod. Biorefin.* **2011**, *5*, 198–214. [CrossRef]
31. Chang, C.; Ma, X.; Cen, P. Kinetics of Levulinic Acid Formation from Glucose Decomposition at High Temperature. *Chin. J. Chem. Eng.* **2006**, *14*, 708–712. [CrossRef]
32. Dutta, S.; Yu, I.K.M.; Tsang, D.C.W.; Ng, Y.H.; Ok, Y.S.; Sherwood, J.; Clark, J.H. Green Synthesis of Gamma-Valerolactone (GVL) through Hydrogenation of Biomass-Derived Levulinic Acid Using Non-Noble Metal Catalysts: A Critical Review. *Chem. Eng. J.* **2019**, *372*, 992–1006. [CrossRef]
33. Abdelrahman, O.A.; Heyden, A.; Bond, J.Q. Analysis of Kinetics and Reaction Pathways in the Aqueous-Phase Hydrogenation of Levulinic Acid to Form γ-Valerolactone over Ru/C. *ACS Catal.* **2014**, *4*, 1171–1181. [CrossRef]
34. Yan, Z.P.; Lin, L.; Liu, S. Synthesis of γ-Valerolactone by Hydrogenation of Biomass- DerivedLevulinic Acid over Ru/C Catalyst. *Energy Fuels* **2009**, *23*, 3853–3858. [CrossRef]
35. Cao, R.; Xin, J.; Zhang, Z.; Liu, Z.; Lu, X.; Ren, B.; Zhang, S. Efficient Conversion of α-Angelica Lactone into γ-Valerolactone with Ionic Liquids at Room Temperature. *ACS Sustain. Chem. Eng.* **2014**, *2*, 902–909. [CrossRef]
36. Upare, P.P.; Lee, J.M.; Hwang, D.W.; Halligudi, S.B.; Hwang, Y.K.; Chang, J.S. Selective Hydrogenation of Levulinic Acid to γ-Valerolactone over Carbon-Supported Noble Metal Catalysts. *J. Ind. Eng. Chem.* **2011**, *17*, 287–292. [CrossRef]
37. Hijazi, A.; Khalaf, N.; Kwapinski, W.; Leahy, J.J. Catalytic Valorisation of Biomass Levulinic Acid into Gamma Valerolactone Using Formic Acid as a H_2 Donor: A Critical Review. *RSC Adv.* **2022**, *12*, 13673–13694. [CrossRef]
38. Ftouni, J.; Genuino, H.C.; Muñoz-Murillo, A.; Bruijnincx, P.C.A.; Weckhuysen, B.M. Influence of Sulfuric Acid on the Performance of Ruthenium-Based Catalysts in the Liquid-Phase Hydrogenation of Levulinic Acid to γ-Valerolactone. *ChemSusChem* **2017**, *10*, 2891–2896. [CrossRef]
39. Braden, D.J.; Henao, C.A.; Heltzel, J.; Maravelias, C.C.; Dumesic, J.A. Production of Liquid Hydrocarbon Fuels by Catalytic Conversion of Biomass-Derived Levulinic Acid. *Green Chem.* **2011**, *13*, 1755–1765. [CrossRef]
40. Genuino, H.C.; Van De Bovenkamp, H.H.; Wilbers, E.; Winkelman, J.G.M.; Goryachev, A.; Hofmann, J.P.; Hensen, E.J.M.; Weckhuysen, B.M.; Bruijnincx, P.C.A.; Heeres, H.J. Catalytic Hydrogenation of Renewable Levulinic Acid to γ-Valerolactone: Insights into the Influence of Feed Impurities on Catalyst Performance in Batch and Flow Reactors. *ACS Sustain. Chem. Eng.* **2020**, *8*, 5903–5919. [CrossRef]

41. Wachała, M.; Grams, J.; Kwapiński, W.; Ruppert, A.M. Influence of ZrO_2 on Catalytic Performance of Ru Catalyst in Hydrolytic Hydrogenation of Cellulose towards γ-Valerolactone. *Int. J. Hydrogen Energy* **2016**, *41*, 8688–8695. [CrossRef]
42. Soszka, E.; Sneka-Płatek, O.; Skiba, E.; Maniukiewicz, W.; Pawlaczyk, A.; Rogowski, J.; Szynkowska-Jóźwik, M.; Ruppert, A.M. Influence of the Presence of Impurities and of the Biomass Source on the Performance of Ru Catalysts in the Hydrolytic Hydrogenation of Cellulose towards γ-Valerolactone. *Fuel* **2022**, *319*, 123646. [CrossRef]
43. Ruppert, A.M.; Grams, J.; Matras-Michalska, J.; Chełmicka, M.; Przybysz, P. ToF-SIMS Study of the Surface of Catalysts Used in Biomass Valorization. *Surf. Interface Anal.* **2014**, *46*, 726–730. [CrossRef]
44. Deng, L.; Zhao, Y.; Li, J.; Fu, Y.; Liao, B.; Guo, Q.X. Conversion of Levulinic Acid and Formic Acid into γ-Valerolactone over Heterogeneous Catalysts. *ChemSusChem* **2010**, *3*, 1172–1175. [CrossRef]
45. Ma, L.; Xiao, T.; Ning, Z.; Liu, Y.; Chen, H.; Peng, J. Pollution and Health Risk Assessment of Toxic Metal(Loid)s in Soils under Different Land Use in Sulphide Mineralized Areas. *Sci. Total Environ.* **2020**, *724*, 138176. [CrossRef]
46. Favas, P.J.C.; Pratas, J.; Varun, M.; D'Souza, R.; Paul, M.S. Phytoremediation of Soils Contaminated with Metals and Metalloids at Mining Areas: Potential of Native Flora. In *Environmental Risk Assessment of Soil Contamination*; Hernandez-Soriano, M.C., Ed.; IntechOpen Ltd.: London, UK, 2014; ISBN 978-953-51-1235-8. [CrossRef]
47. Etim, E.E. Phytoremediation and Its Mechanisms: A Review. *Int. J. Environ. Bioenergy* **2012**, *2*, 120–136.
48. Caillat, S.; Vakkilainen, E. *Large-Scale Biomass Combustion Plants: An Overview*; Woodhead Publishing Limited: Sawston, UK, 2013; ISBN 9780857091314.
49. Chen, K.; Ng, K.H.; Cheng, C.K.; Cheng, Y.W.; Chong, C.C.; Vo, D.V.N.; Witoon, T.; Ismail, M.H. Biomass-Derived Carbon-Based and Silica-Based Materials for Catalytic and Adsorptive Applications—An Update since 2010. *Chemosphere* **2022**, *287*, 132222. [CrossRef]
50. Rachniyom, W.; Srisittipokakun, N.; Kaewkhao, J. Comparative Study of SiO_2 in Biomass Ashes at Different Temperatures. *Interdiscip. Res. Rev.* **2019**, *14*, 12–15. [CrossRef]
51. Vassilev, S.V.; Baxter, D.; Andersen, L.K.; Vassileva, C.G. An Overview of the Composition and Application of Biomass Ash. Part 1. Phase-Mineral and Chemical Composition and Classification. *Fuel* **2013**, *105*, 40–76. [CrossRef]
52. Chen, H.; Yu, B.; Jin, S. Production of Levulinic Acid from Steam Exploded Rice Straw via Solid Superacid, S_2O_{82}-/ZrO_2-SiO_2-Sm_2O_3. *Bioresour. Technol.* **2011**, *102*, 3568–3570. [CrossRef] [PubMed]
53. Pająk, M.; Halecki, W.; Gąsiorek, M. Accumulative Response of Scots Pine (*Pinus sylvestris* L.) and Silver Birch (*Betula pendula* Roth) to Heavy Metals Enhanced by Pb-Zn Ore Mining and Processing Plants: Explicitly Spatial Considerations of Ordinary Kriging Based on a GIS Approach. *Chemosphere* **2017**, *168*, 851–859. [CrossRef]
54. Fachri, B.A.; Abdilla, R.M.; De Bovenkamp, H.H.V.; Rasrendra, C.B.; Heeres, H.J. Experimental and Kinetic Modeling Studies on the Sulfuric Acid Catalyzed Conversion of d -Fructose to 5-Hydroxymethylfurfural and Levulinic Acid in Water. *ACS Sustain. Chem. Eng.* **2015**, *3*, 3024–3034. [CrossRef]
55. Pang, J.; Zheng, M.; Sun, R.; Song, L.; Wang, A.; Wang, X.; Zhang, T. Catalytic Conversion of Cellulosic Biomass to Ethylene Glycol: Effects of Inorganic Impurities in Biomass. *Bioresour. Technol.* **2015**, *175*, 424–429. [CrossRef] [PubMed]
56. Cao, X.; Peng, X.; Sun, S.; Zhong, L.; Chen, W.; Wang, S.; Sun, R.C. Hydrothermal Conversion of Xylose, Glucose, and Cellulose under the Catalysis of Transition Metal Sulfates. *Carbohydr. Polym.* **2015**, *118*, 44–51. [CrossRef]
57. Paniagua, M.; Morales, G.; Melero, J.A.; García-Salgado, D. Insights into the Influence of Feed Impurities on Catalytic Performance in the Solvent-Free Dimerization of Renewable Levulinic Acid. *Catal. Today* **2024**, *428*, 114446. [CrossRef]
58. Zeng, M.; Pan, X. Insights into Solid Acid Catalysts for Efficient Cellulose Hydrolysis to Glucose: Progress, Challenges, and Future Opportunities. *Catal. Rev.—Sci. Eng.* **2022**, *64*, 445–490. [CrossRef]
59. Tang, P.; Yu, J. Kinetic Analysis on Deactivation of a Solid Brønsted Acid Catalyst in Conversion of Sucrose to Levulinic Acid. *Ind. Eng. Chem. Res.* **2014**, *53*, 11629–11637. [CrossRef]
60. Lin, F.; Xu, M.; Ramasamy, K.K.; Li, Z.; Klinger, J.L.; Schaidle, J.A.; Wang, H. Catalyst Deactivation and Its Mitigation during Catalytic Conversions of Biomass. *ACS Catal.* **2022**, *12*, 13555–13599. [CrossRef]
61. Potvin, J.; Sorlien, E.; Hegner, J.; DeBoef, B.; Lucht, B.L. Effect of NaCl on the Conversion of Cellulose to Glucose and Levulinic Acid via Solid Supported Acid Catalysis. *Tetrahedron Lett.* **2011**, *52*, 5891–5893. [CrossRef]
62. Kang, S.; Fu, J.; Zhang, G. From Lignocellulosic Biomass to Levulinic Acid: A Review on Acid-Catalyzed Hydrolysis. *Renew. Sustain. Energy Rev.* **2018**, *94*, 340–362. [CrossRef]
63. Zareihassangheshlaghi, A.; Dizaji, H.B.; Zeng, T.; Huth, P.; Ruf, T.; Denecke, R.; Enke, D. Behavior of Metal Impurities on Surface and Bulk of Biogenic Silica from Rice Husk Combustion and the Impact on Ash-Melting Tendency. *ACS Sustain. Chem. Eng.* **2020**, *8*, 10369–10379. [CrossRef]
64. Lee, J.; Saha, B.; Vlachos, D.G. Pt Catalysts for Efficient Aerobic Oxidation of Glucose to Glucaric Acid in Water. *Green Chem.* **2016**, *18*, 3815–3822. [CrossRef]
65. Borg, Ø.; Hammer, N.; Enger, B.C.; Myrstad, R.; Lindvg, O.A.; Eri, S.; Skagseth, T.H.; Rytter, E. Effect of Biomass-Derived Synthesis Gas Impurity Elements on Cobalt Fischer-Tropsch Catalyst Performance Including in Situ Sulphur and Nitrogen Addition. *J. Catal.* **2011**, *279*, 163–173. [CrossRef]
66. Mthembu, L.D.; Gupta, R.; Dziike, F.; Lokhat, D.; Deenadayalu, N. Conversion of Biomass-Derived Levulinic Acid into γ-Valerolactone Using Methanesulfonic Acid: An Optimization Study Using Response Surface Methodology. *Fermentation* **2023**, *9*, 288. [CrossRef]

67. Ren, Q.; Zhao, C. Evolution of Fuel-N in Gas Phase during Biomass Pyrolysis. *Renew. Sustain. Energy Rev.* **2015**, *50*, 408–418. [CrossRef]
68. Baker, L.A.; Habershon, S. Photosynthetic Pigment-Protein Complexes as Highly Connected Networks: Implications for Robust Energy Transport. *Proc. R. Soc. A Math. Phys. Eng. Sci.* **2017**, *473*, 20170112. [CrossRef] [PubMed]
69. Schwartz, T.J.; Johnson, R.L.; Cardenas, J.; Okerlund, A.; Da Silva, N.A.; Schmidt-Rohr, K.; Dumesic, J.A. Engineering Catalyst Microenvironments for Metal-Catalyzed Hydrogenation of Biologically Derived Platform Chemicals. *Angew. Chem.—Int. Ed.* **2014**, *53*, 12718–12722. [CrossRef] [PubMed]
70. Zhang, Z.; Jackson, J.E.; Miller, D.J. Effect of Biogenic Fermentation Impurities on Lactic Acid Hydrogenation to Propylene Glycol. *Bioresour. Technol.* **2008**, *99*, 5873–5880. [CrossRef]
71. Ruppert, A.M.; Jędrzejczyk, M.; Sneka-Płatek, O.; Keller, N.; Dumon, A.S.; Michel, C.; Sautet, P.; Grams, J. Ru Catalysts for Levulinic Acid Hydrogenation with Formic Acid as a Hydrogen Source. *Green Chem.* **2016**, *18*, 2014–2028. [CrossRef]
72. Wojciechowska, J.; Jędrzejczyk, M.; Grams, J.; Keller, N.; Ruppert, A.M. Enhanced Production of Γ-Valerolactone with an Internal Source of Hydrogen on Ca-Modified TiO_2 Supported Ru Catalysts. *ChemSusChem* **2019**, *12*, 639–650. [CrossRef]
73. Ruppert, A.M.; Jędrzejczyk, M.; Potrzebowska, N.; Kaźmierczak, K.; Brzezińska, M.; Sneka-Płatek, O.; Sautet, P.; Keller, N.; Michel, C.; Grams, J. Supported Gold-Nickel Nano-Alloy as a Highly Efficient Catalyst in Levulinic Acid Hydrogenation with Formic Acid as an Internal Hydrogen Source. *Catal. Sci. Technol.* **2018**, *8*, 4318–4331. [CrossRef]
74. Sneka-Płatek, O.; Kaźmierczak, K.; Jędrzejczyk, M.; Sautet, P.; Keller, N.; Michel, C.; Ruppert, A.M. Understanding the Influence of the Composition of the Ag[Sbnd]Pd Catalysts on the Selective Formic Acid Decomposition and Subsequent Levulinic Acid Hydrogenation. *Int. J. Hydrogen Energy* **2020**, *45*, 17339–17353. [CrossRef]
75. Mohan, V.; Raghavendra, C.; Pramod, C.V.; Raju, B.D.; Rama Rao, K.S. Ni/H-ZSM-5 as a Promising Catalyst for Vapour Phase Hydrogenation of Levulinic Acid at Atmospheric Pressure. *RSC Adv.* **2014**, *4*, 9660–9668. [CrossRef]
76. Varkolu, M.; Raju Burri, D.; Rao Kamaraju, S.R.; Jonnalagadda, S.B.; van Zyl, W.E. Hydrogenation of Levulinic Acid Using Formic Acid as a Hydrogen Source over Ni/SiO_2 Catalysts. *Chem. Eng. Technol.* **2017**, *40*, 719–726. [CrossRef]
77. Guo, H.; Wang, G.; Zhang, B.; Li, J.; Sui, W.; Jia, H.; Si, C. Ultrafine Ru Nanoparticles Deposited on Lignin-Derived Nitrogen-Doped Carbon Nanolayer for the Efficient Conversion of Levulinic Acid to γ-Valerolactone. *Renew. Energy* **2024**, *222*, 119954. [CrossRef]
78. Grillo, G.; Manzoli, M.; Bucciol, F.; Tabasso, S.; Tabanelli, T.; Cavani, F.; Cravotto, G. Hydrogenation of Levulinic Acid to γ-Valerolactone via Green Microwave-Assisted Reactions Either in Continuous Flow or Solvent-Free Batch Processes. *Ind. Eng. Chem. Res.* **2021**, *60*, 16756–16768. [CrossRef]
79. Schwartz, T.J.; O'Neill, B.J.; Shanks, B.H.; Dumesic, J.A. Bridging the Chemical and Biological Catalysis Gap: Challenges and Outlooks for Producing Sustainable Chemicals. *ACS Catal.* **2014**, *4*, 2060–2069. [CrossRef]
80. König, C.F.J.; Schuh, P.; Huthwelker, T.; Smolentsev, G.; Schildhauer, T.J.; Nachtegaal, M. Influence of the Support on Sulfur Poisoning and Regeneration of Ru Catalysts Probed by Sulfur K-Edge X-ray Absorption Spectroscopy. *Catal. Today* **2014**, *229*, 56–63. [CrossRef]
81. Arena, B.J. Deactivation of Ruthenium Catalysts in Continuous Glucose Hydrogenation. *Appl. Catal. A Gen.* **1992**, *87*, 219–229. [CrossRef]
82. te Molder, T.D.J.; Kersten, S.R.A.; Lange, J.P.; Ruiz, M.P. Do Not Forget the Classical Catalyst Poisons: The Case of Biomass to Glycols via Catalytic Hydrogenolysis. *Biofuels Bioprod. Biorefin.* **2022**, *16*, 1274–1283. [CrossRef]
83. Sitotaw, Y.W.; Habtu, N.G.; Gebreyohannes, A.Y.; Nunes, S.P.; Van Gerven, T. Ball Milling as an Important Pretreatment Technique in Lignocellulose Biorefineries: A Review. *Biomass Convers. Biorefin.* **2021**, *13*, 15593–15616. [CrossRef]
84. Mayer-Laigle, C.; Rajaonarivony, R.K.; Blanc, N.; Rouau, X. Comminution of Dry Lignocellulosic Biomass: Part II. Technologies, Improvement of Milling Performances, and Security Issues. *Bioengineering* **2018**, *5*, 50. [CrossRef]
85. Di Nardo, T.; Moores, A. Mechanochemical Amorphization of Chitin: Impact of Apparatus Material on Performance and Contamination. *Beilstein J. Org. Chem.* **2019**, *15*, 1217–1225. [CrossRef]
86. Besson, M.; Gallezot, P. Deactivation of Metal Catalysts in Liquid Phase Organic Reactions. *Catal. Today* **2003**, *81*, 547–559. [CrossRef]
87. Kusserow, B.; Schimpf, S.; Claus, P. Hydrogenation of Glucose to Sorbitol over Nickel and Ruthenium Catalysts. *Adv. Synth. Catal.* **2003**, *345*, 289–299. [CrossRef]
88. Van Zandvoort, I.; Wang, Y.; Rasrendra, C.B.; Van Eck, E.R.H.; Bruijnincx, P.C.A.; Heeres, H.J.; Weckhuysen, B.M. Formation, Molecular Structure, and Morphology of Humins in Biomass Conversion: Influence of Feedstock and Processing Conditions. *ChemSusChem* **2013**, *6*, 1745–1758. [CrossRef] [PubMed]
89. Patil, S.K.R.; Lund, C.R.F. Formation and Growth of Humins via Aldol Addition and Condensation during Acid-Catalyzed Conversion of 5-Hydroxymethylfurfural. *Energy Fuels* **2011**, *25*, 4745–4755. [CrossRef]
90. Sievers, C.; Valenzuela-Olarte, M.B.; Marzialetti, T.; Musin, I.; Agrawal, P.K.; Jones, C.W. Ionic-Liquid-Phase Hydrolysis of Pine Wood. *Ind. Eng. Chem. Res.* **2009**, *48*, 1277–1286. [CrossRef]
91. Weingarten, R.; Cho, J.; Conner, W.C.; Huber, G.W. Kinetics of Furfural Production by Dehydration of Xylose in a Biphasic Reactor with Microwave Heating. *Green Chem.* **2010**, *12*, 1423–1429. [CrossRef]
92. Koranchalil, S.; Nielsen, M. Direct Biomass Valorisation to C-Valerolactone by Ru-PNP Catalysed Hydrogenation in Acid. *EES Catal.* 2024; Advance Article. [CrossRef]

93. Liu, S.; Zhu, Y.; Liao, Y.; Wang, H.; Liu, Q.; Ma, L.; Wang, C. Advances in Understanding the Humins: Formation, Prevention and Application. *Appl. Energy Combust. Sci.* **2022**, *10*, 100062. [CrossRef]
94. Wettstein, S.G.; Alonso, D.M.; Chong, Y.; Dumesic, J.A. Production of Levulinic Acid and Gamma-Valerolactone (GVL) from Cellulose Using GVL as a Solvent in Biphasic Systems. *Energy Environ. Sci.* **2012**, *5*, 8199–8203. [CrossRef]
95. Alonso, D.M.; Gallo, J.M.R.; Mellmer, M.A.; Wettstein, S.G.; Dumesic, J.A. Direct Conversion of Cellulose to Levulinic Acid and Gamma-Valerolactone Using Solid Acid Catalysts. *Catal. Sci. Technol.* **2013**, *3*, 927–931. [CrossRef]
96. Son, P.A.; Nishimura, S.; Ebitani, K. Production of γ-Valerolactone from Biomass-Derived Compounds Using Formic Acid as a Hydrogen Source over Supported Metal Catalysts in Water Solvent. *RSC Adv.* **2014**, *4*, 10525–10530. [CrossRef]
97. Du, S.; Gamliel, D.P.; Giotto, M.V.; Valla, J.A.; Bollas, G.M. Coke Formation of Model Compounds Relevant to Pyrolysis Bio-Oil over ZSM-5. *Appl. Catal. A Gen.* **2016**, *513*, 67–81. [CrossRef]
98. Pritchard, A.M. *The Economics of Fouling*; Springer: Dordrecht, The Nerthlands, 1987; ISBN 9788578110796.
99. Bartholomew, C.H. Mechanisms of Catalyst Deactivation. *Appl. Catal. A Gen.* **2001**, *212*, 17–60. [CrossRef]
100. Varkolu, M.; Velpula, V.; Burri, D.R.; Kamaraju, S.R.R. Gas Phase Hydrogenation of Levulinic Acid to γ-Valerolactone over Supported Ni Catalysts with Formic Acid as Hydrogen Source. *New J. Chem.* **2016**, *40*, 3261–3267. [CrossRef]
101. Yu, Z.; Lu, X.; Bai, H.; Xiong, J.; Feng, W.; Ji, N. Effects of Solid Acid Supports on the Bifunctional Catalysis of Levulinic Acid to γ-Valerolactone: Catalytic Activity and Stability. *Chem.—Asian J.* **2020**, *15*, 1182–1201. [CrossRef] [PubMed]
102. Girisuta, B.; Janssen, L.P.B.M.; Heeres, H.J. A Kinetic Study on the Decomposition of 5-Hydroxymethylfurfural into Levulinic Acid. *Green Chem.* **2006**, *8*, 701–709. [CrossRef]
103. Aguayo, A.T.; Gayubo, A.G.; Atutxa, A.; Olazar, M.; Bilbao, J. Catalyst Deactivation by Coke in the Transformation of Aqueous Ethanol into Hydrocarbons. Kinetic Modeling and Acidity Deterioration of the Catalyst. *Ind. Eng. Chem. Res.* **2002**, *41*, 4216–4224. [CrossRef]
104. Sahoo, S.K.; Viswanadham, N.; Ray, N.; Gupta, J.K.; Singh, I.D. Studies on Acidity, Activity and Coke Deactivation of ZSM-5 during n-Heptane Aromatization. *Appl. Catal. A Gen.* **2001**, *205*, 1–10. [CrossRef]
105. Putro, J.N.; Kurniawan, A.; Soetaredjo, F.E.; Lin, S.Y.; Ju, Y.H.; Ismadji, S. Production of Gamma-Valerolactone from Sugarcane Bagasse over TiO_2-Supported Platinum and Acid-Activated Bentonite as a Co-Catalyst. *RSC Adv.* **2015**, *5*, 41285–41299. [CrossRef]
106. Kondeboina, M.; Enumula, S.S.; Reddy, K.S.; Challa, P.; Burri, D.R.; Kamaraju, S.R.R. Bimetallic Ni-Co/γ-Al_2O_3 Catalyst for Vapour Phase Production of γ-Valerolactone: Deactivation Studies and Feedstock Selection. *Fuel* **2021**, *285*, 119094. [CrossRef]
107. Serrano-Ruiz, J.C.; Pineda, A.; Balu, A.M.; Luque, R.; Campelo, J.M.; Romero, A.A.; Ramos-Fernández, J.M. Catalytic Transformations of Biomass-Derived Acids into Advanced Biofuels. *Catal. Today* **2012**, *195*, 162–168. [CrossRef]
108. Luo, W.; Deka, U.; Beale, A.M.; Van Eck, E.R.H.; Bruijnincx, P.C.A.; Weckhuysen, B.M. Ruthenium-Catalyzed Hydrogenation of Levulinic Acid: Influence of the Support and Solvent on Catalyst Selectivity and Stability. *J. Catal.* **2013**, *301*, 175–186. [CrossRef]
109. Cao, W.; Luo, W.; Ge, H.; Su, Y.; Wang, A.; Zhang, T. UiO-66 Derived Ru/ZrO_2@C as a Highly Stable Catalyst for Hydrogenation of Levulinic Acid to γ-Valerolactone. *Green Chem.* **2017**, *19*, 2201–2211. [CrossRef]
110. Wettstein, S.G.; Bond, J.Q.; Alonso, D.M.; Pham, H.N.; Datye, A.K.; Dumesic, J.A. RuSn Bimetallic Catalysts for Selective Hydrogenation of Levulinic Acid to γ-Valerolactone. *Appl. Catal. B Environ.* **2012**, *117–118*, 321–329. [CrossRef]
111. Banerjee, B.; Singuru, R.; Kundu, S.K.; Dhanalaxmi, K.; Bai, L.; Zhao, Y.; Reddy, B.M.; Bhaumik, A.; Mondal, J. Towards Rational Design of Core-Shell Catalytic Nanoreactor with High Performance Catalytic Hydrogenation of Levulinic Acid. *Catal. Sci. Technol.* **2016**, *6*, 5102–5115. [CrossRef]
112. Zhou, H.; Song, J.; Kang, X.; Hu, J.; Yang, Y.; Fan, H.; Meng, Q.; Han, B. One-Pot Conversion of Carbohydrates into Gamma-Valerolactone Catalyzed by Highly Cross-Linked Ionic Liquid Polymer and Co/TiO_2. *RSC Adv.* **2015**, *5*, 15267–15273. [CrossRef]
113. Boddula, R.; Shanmugam, P.; Srivatsava, R.K.; Tabassum, N.; Pothu, R.; Naik, R.; Saran, A.; Viswanadham, B.; Radwan, A.B.; Al-Qahtani, N. Catalytic Valorisation of Biomass-Derived Levulinic Acid to Biofuel Additive γ-Valerolactone: Influence of Copper Loading on Silica Support. *Reactions* **2023**, *4*, 465–477. [CrossRef]
114. Hussain, S.K.; Velisoju, V.K.; Rajan, N.P.; Kumar, B.P.; Chary, K.V.R. Synthesis of γ-Valerolactone from Levulinic Acid and Formic Acid over Mg-Al Hydrotalcite Like Compound. *ChemistrySelect* **2018**, *3*, 6186–6194. [CrossRef]
115. Kumar, V.V.; Naresh, G.; Sudhakar, M.; Anjaneyulu, C.; Bhargava, S.K.; Tardio, J.; Reddy, V.K.; Padmasri, A.H.; Venugopal, A. An Investigation on the Influence of Support Type for Ni Catalysed Vapour Phase Hydrogenation of Aqueous Levulinic Acid to γ-Valerolactone. *RSC Adv.* **2016**, *6*, 9872–9879. [CrossRef]
116. Putrakumar, B.; Nagaraju, N.; Kumar, V.P.; Chary, K.V.R. Hydrogenation of Levulinic Acid to γ-Valerolactone over Copper Catalysts Supported on γ-Al_2O_3. *Catal. Today* **2015**, *250*, 209–217. [CrossRef]
117. Wang, J.; Jaenicke, S.; Chuah, G.K. Zirconium-Beta Zeolite as a Robust Catalyst for the Transformation of Levulinic Acid to γ-Valerolactone via Meerwein-Ponndorf-Verley Reduction. *RSC Adv.* **2014**, *4*, 13481–13489. [CrossRef]
118. Zhao, R.; Kasipandi, S.; Shin, C.H.; Bae, J.W. Catalytic Conversion of Biomass-Derived Levulinic Acid to γ-Valerolactone over Amphoteric Zirconium Hydroxide. *ACS Catal.* **2023**, *13*, 12711–12722. [CrossRef]